AD-A071 018 ILLINOIS UNIV AT URBANA-CHAMPAIGN ELECTRO-PHYSICS LAB F/G 20/5
MULTIPLE PHOTON PUMPING OF MOLECULAR LASERS: FREQUENCY TUNABLE --ETC(U)
APR 79 P D COLEMAN AFOSR-76-2988
UNCLASSIFIED UILU-ENG-79-2550 AFOSR-TR-79-0738 NL

1 OF 1
AD A071018

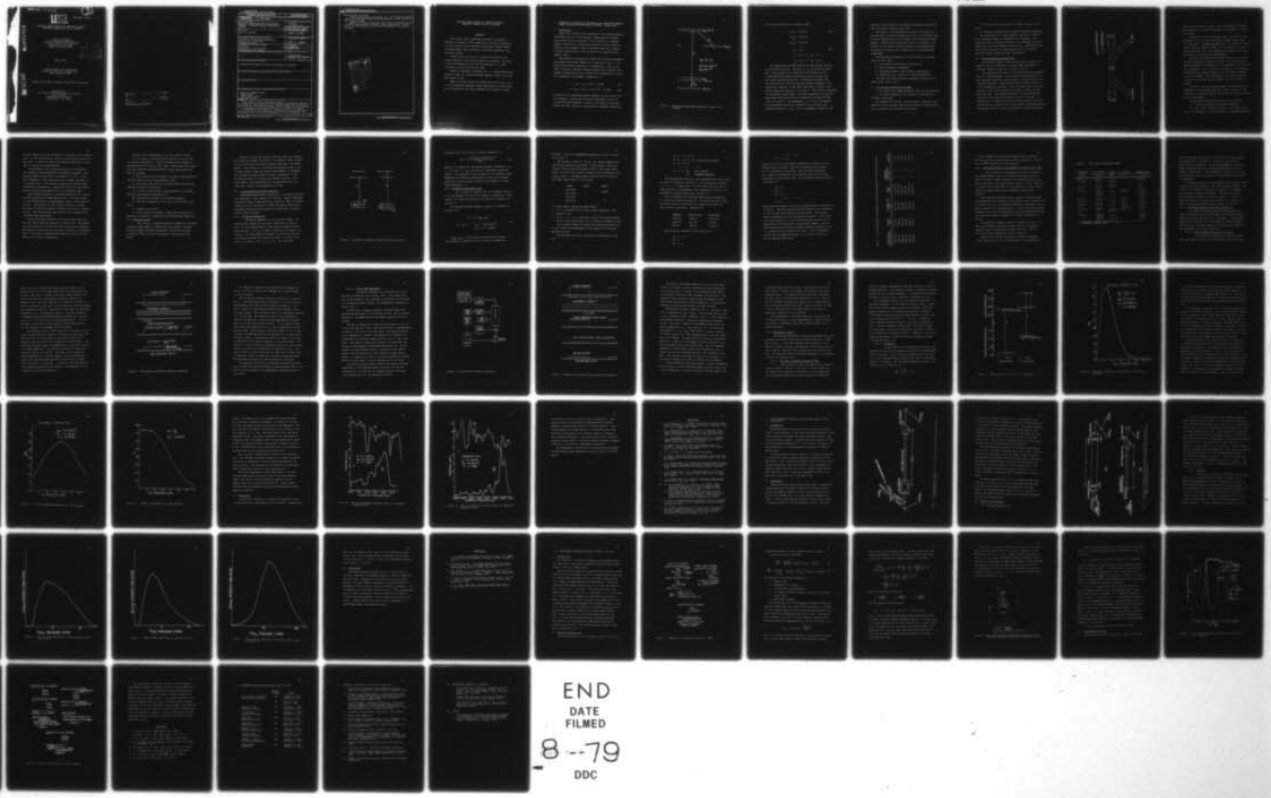

END
DATE FILMED
8-79
DDC

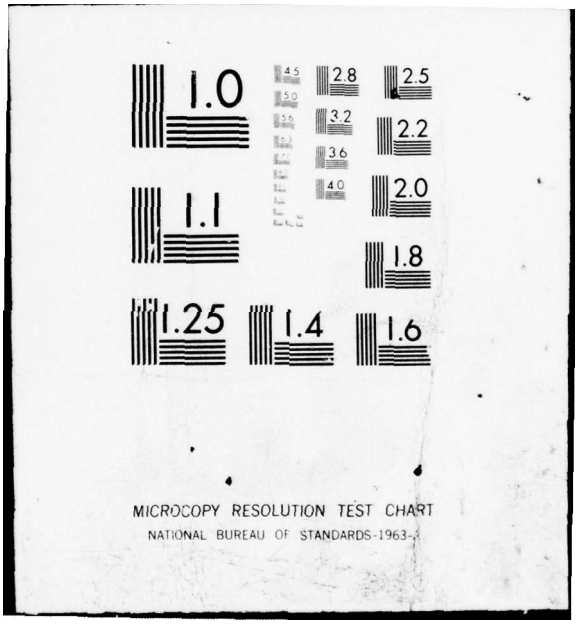
1.0
1.1
1.25
1.4
1.6
1.8
2.0
2.2
2.5
2.8
3.2
3.6
4.0
4.5
5.0
5.6
MICROCOPY RESOLUTION TEST CHART
NATIONAL BUREAU OF STANDARDS-1963-A

AFOSR-TR- 79-0738

(3)

LEVEL

UILU-ENG-79-2550

AD A071018

MULTIPLE PHOTON PUMPING OF MOLECULAR LASERS: FREQUENCY TUNABLE AND FAR IR LASERS

Paul D. Coleman
Electro-Physics Laboratory
Electrical Engineering Department
University of Illinois
Urbana, Illinois 61801

DDC
RECEIVED
JUL 10 1979
C

April 1979

Interim Report for the Period
1 February 1978 to 31 January 1979
Grant AFOSR 76-2988

Approved for public release; distribution unlimited.

DDC FILE COPY

Prepared for
Air Force Office of Scientific Research
Building 410
Bolling Air Force Base
Washington, D.C. 20332

AIR FORCE OFFICE OF SCIENTIFIC RESEARCH (AFSC)
NOTICE OF TRANSMITTAL TO DDC
This technical report has been reviewed and is approved for public release IAW AFR 190-12 (7b).
Distribution is unlimited.
A. D. BLOSE
Technical Information Officer

UNCLASSIFIED

SECURITY CLASSIFICATION OF THIS PAGE (When Data Entered)

REPORT DOCUMENTATION PAGE	READ INSTRUCTIONS BEFORE COMPLETING FORM
1. REPORT NUMBER: AFOSR-TR-79-0738	2. GOVT ACCESSION NO. / 3. RECIPIENT'S CATALOG NUMBER
4. TITLE (and Subtitle): MULTIPLE PHOTON PUMPING OF MOLECULAR LASERS: FREQUENCY TUNABLE AND FAR IR LASERS	5. TYPE OF REPORT & PERIOD COVERED: Interim 2-1-78/1-31-79
	6. PERFORMING ORG. REPORT NUMBER: UILU-ENG-79-2550
7. AUTHOR(s): Paul D. Coleman	8. CONTRACT OR GRANT NUMBER(s): AFOSR 76-2988C
9. PERFORMING ORGANIZATION NAME AND ADDRESS: Electrical Engineering Department, University of Illinois, Urbana, IL 61801	10. PROGRAM ELEMENT, PROJECT, TASK AREA & WORK UNIT NUMBERS: 2301/A1 61102F
11. CONTROLLING OFFICE NAME AND ADDRESS: AFOSR/NP, Building 410, Bolling AFB, Washington, D.C. 20332	12. REPORT DATE: April 1979
	13. NUMBER OF PAGES: 73
14. MONITORING AGENCY NAME & ADDRESS (if different from Controlling Office): Interim rept. 1 Feb 78 - 31 Jan 79	15. SECURITY CLASS. (of this report): Unclassified
	15a. DECLASSIFICATION/DOWNGRADING SCHEDULE

16. DISTRIBUTION STATEMENT (of this Report)

Approved for public release; distribution unlimited.

17. DISTRIBUTION STATEMENT (of the abstract entered in Block 20, if different from Report)

18. SUPPLEMENTARY NOTES

19. KEY WORDS (Continue on reverse side if necessary and identify by block number)

Optically pumped lasers
Raman lasers
hyper-Raman lasers
hot band lasing

20. ABSTRACT (Continue on reverse side if necessary and identify by block number)

This annual report describes research on two-photon pumping of molecular lasers operating on hot band transitions of the molecules and the associated nonlinear effects (Raman and hyper-Raman) that contribute to the gain spectrum of the molecular system.

Accessing the hot bands of a molecule results in more lasing transitions that would otherwise be observed, and modifies the characteristics of the gain spectrum, i.e., the saturation, AC → next page

DD FORM 1 JAN 73 1473 EDITION OF 1 NOV 65 IS OBSOLETE

Unclassified

SECURITY CLASSIFICATION OF THIS PAGE (When Data Entered)

403 714

Stark shifts and width.

Specific experiments described are: a) infrared-microwave pumping of NH_3, b) infrared-infrared pumping of NH_3, and c) hot band lasing in NH_3.

Ammonia has been chosen for study since it has both a rich 10 micron and microwave spectrum, whose spectroscopy is well-known, so that absorption and laser assignements can readily be made.

Accession For
NTIS GRA&I
DDC TAB
Unannounced
Justification
By
Distribution/
Availability Codes
Dist | Avail and/or special
A

MULTIPLE PHOTON PUMPING OF MOLECULAR LASERS: FREQUENCY TUNABLE AND FAR IR LASERS

ABSTRACT

This annual report describes research on two-photon pumping of molecular lasers operating on hot band transitions of the molecules and the associated nonlinear effects (Raman and hyper-Raman) that contribute to the gain spectrum of the molecular system.

Accessing the hot bands of a molecule results in more lasing transitions that would otherwise be observed, and modifies the characteristics of the gain spectrum, i.e., the saturation, AC Stark shifts and width.

Specific experiments described are: a) infrared-microwave pumping of NH_3, b) infrared-infrared pumping of NH_3, and c) hot band lasing in NH_3.

Ammonia has been chosen for study since it has both a rich 10 μm and microwave spectrum, whose spectroscopy is well-known, so that absorption and laser assignments can readily be made.

1. GENERATION OF TUNABLE FAR INFRARED USING INFRARED-MICROWAVE PUMPED STIMULATED HYPER-RAMAN SCATTERING - Edward Malk

I. Introduction

Tunable Far Infrared (FIR) generation, using optical pumping techniques, has yet to be achieved. Demonstration of Raman type transitions has occurred[1,2,3] but the lack of a tunable pumping source has not permitted the desired tunable emission. Multiple photon pumping using an infrared laser and a tunable microwave source offers a way to achieve the desired tunable pumping quanta.

The process to produce the tunable FIR is called Stimulated Hyper-Raman Scattering[4] (SHRS) and is depicted in Fig. 1. Infrared and microwave radiations at frequencies ν_ℓ and ν_m are used to optically pump the indicated energy level system. The pumping frequencies are near resonant with the molecular transition frequencies, as defined in Equation (1).

$$\Delta\nu = \Omega_{01} - \nu_m < 0.5 \text{ cm}^{-1} \text{ (15 GHz)} \qquad \text{(1a)}$$

$$\delta\nu = \Omega_{03} - (\nu_m + \nu_\ell) < 0.05 \text{ cm}^{-1} \text{ (1.5 GHz)} \qquad \text{(1b)}$$

A result of the infrared-microwave pumping[5] is gain at the signal frequency ν_s which has three basic components, each with a characteristic frequency. Equation (2a) shows the gain components and (2b) gives the characteristic frequency, neglecting

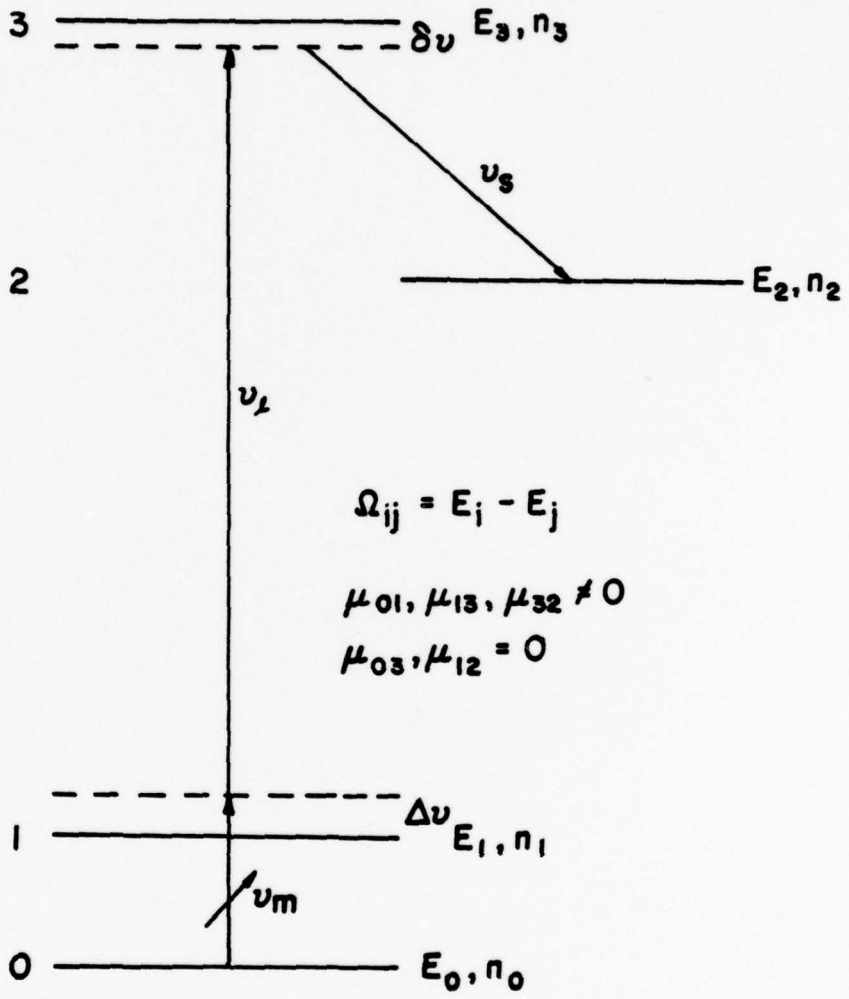

Figure 1. Stimulated hyper-Raman scattering energy level diagram.

any AC Stark shifting of the energy levels.

$$g(\nu_{s_1}) \propto A(n_3-n_2) \tag{2a}$$

$$g(\nu_{s_2}) \propto C(n_1-n_2)$$

$$g(\nu_{s_3}) \propto D(n_0-n_2)$$

$$\nu_{s_1} \approx \Omega_{32} \tag{2b}$$

$$\nu_{s_2} \approx \Omega_{12} - \nu_\ell = \Omega_{32} - \Delta\nu - \delta\nu$$

$$\nu_{s_3} \approx \Omega_{32} - \delta\nu = \Omega_{02} - (\nu_m + \nu_\ell)$$

The components are identified by the populations involved in calculating the gain. The gain at ν_{s_1} is called the laser gain. The systems to be studied are non-resonant for the linear pumping and nearly resonant for the non-linear case. The linear pumping contribution is therefore neglected, and the laser gain only results from the two-photon pumping. The second gain component is the Raman term which involves a two-photon transition from level 1 to level 2. This term is neglected for the reason stated above. The final component is called the Hyper-Raman term and involves a three-photon transition from level 0 to level 2. The frequency, ν_{s_3}, of this term depends on the molecular transition frequency, Ω_{02}, and the input pumping frequencies ν_ℓ and ν_m as is expressed in Equation (2b).

Therefore tuning either of the pumping frequencies effectively tunes the signal frequency gain curve.

The theory of this phenomenon has been the subject of an investigation by Kim and Coleman[5] and will not be detailed here. Following demonstration of the effect using infrared-microwave pumping, a detailed re-investigation will be considered. The subject of this report concerns progress in the experimental realization of tunable far infrared using infrared-microwave pumped SHRS.

The experimental approach to this problem can be broken down into four steps:

1) Cell design and molecular system choice,

2) Double-resonance experiments,

3) Infrared-microwave optical pumping experiments,

4) Demonstration of tunable far infrared generation.

The first two steps have been completed and work is currently under way on step 3.

II. Cell Designs and Molecular System

A cell design for a SHRS experiment requires the following:

1) Collinear propagation of infrared, far infrared and microwave radiations.

2) Feedback for the FIR. The non-linear experiments proposed may have relatively small gains and hence a FIR resonator may be required for the desirable emissions.

3) The cell will be operated at a modest vacuum ($\sim 10^{-4}$ torr).

4) Molecular system dictates useable microwave frequencies.

The availability of 35 GHz equipment has led to a search for a molecular system to accomodate this frequency. The search for such a molecular system will be described following discussion of the cell designs used thus far. Experimental results using the cells will be presented with the infrared-microwave double resonance (IMDR) experiments.

II.1 Waveguide Double-Resonance Cell

The waveguide double resonance cell does not permit FIR feedback but was constructed to perform IMDR experiments. A schematic diagram of the cell is shown in Fig. 2.

The operating principles of the waveguide double-resonance cell are straightforward. The microwaves from the source in a TE_{10} waveguide mode and encounter the 45° H-plane junction with a similar waveguide. The direction angle stated is relative to the propagation direction. The five wires are in line with one wall of the inital waveguide and serve to short the 135° direction path. The incident radiation is therefore guided around the 45° corner at relatively low loss (<0.5 dB). A straight path is obtained for the infrared radiation, with the wires serving to scatter some of the incident infrared radiation. This design allows for easily obtainable collinear propagation

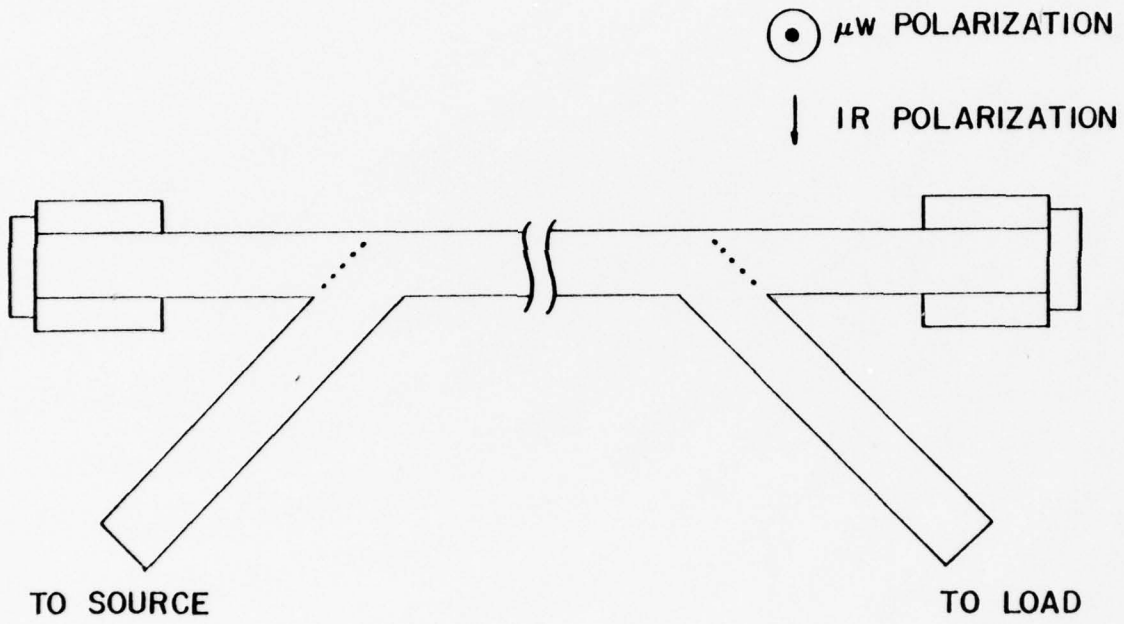

Figure 2. Waveguide double resonance cell.

of the microwaves and infrared. The wires present a sizeable diffraction loss for the FIR and are not desirable in a resonator design.

A microwave Klystron (OKI-35V10) with a slotted line was attached to the "to source" port and a matched load to the "to load" port. The measured VSWR was <1.5 in the 33 to 35 GHz range. This was improved (VSWR <1.1) by addition of a stub tuner before the cell. The transmission spectrum of the cell was found to be relatively structureless.

The CO_2 laser radiation is passed through one of the KCl windows and detected through the other. The infrared transmission through the evacuated cell was measured to be about 75%. The transmission loss is caused by the wires in the waveguide scattering the incident radiation, and the normal incidence to the KCl windows. The transmission loss should also be a function of the input focusing optics, but has not been examined.

Microwave radiation leakage through the KCl windows was measured to be 30 dB down from the incident radiation. Because of the technique used to measure it, the actual leakage may be much larger.

The desirable characteristics of the cell include:

1) linear polarization of microwave radiation,

2) cell length is easily variable. The length of the cell is determined by a straight section of waveguide between

the end pieces. The flanges are not shown in Fig. 2.

3) high vacuum cell easily obtainable,

4) collinear infrared-microwave propagation easily obtained.

The best IMDR experimental results have been achieved using the Waveguide Double resonance cell, as will be seen later.

II-2 Resonator Cell

The resonator cell design offers collinear propagation of the three radiations with an 8 millimeter free aperture for the FIR resonator. This design is considerably more complex than the waveguide double resonance cell. A somewhat similar design has been made by H. Jones[6] for IMDR experiments.

A diagram for half of the cell is shown in Fig. 3. The other half is nearly identical to half shown. A salt window mounted at Brewster's angle replaces the silicon vacuum window (B), and vacuum connections are made to the other mirror mount.

The microwave radiation is introduced through standard 35 GHz waveguide (RG-96) from either port and travels through a transition to standard 10 GHz waveguide (RG-52). The change in boundary conditions causes higher order modes of the 35 GHz to be excited. The radiation makes a bend and encounters the 10 mm Teflon tubing, again causing higher order modes to be excited. A transition from the rectangular waveguide (0.4"× 0.9") to circular (0.4" ID) waveguide forces the microwaves to propagate down the axis of the Teflon tube. Once the radiation is through the circular guide the reverse process occurs

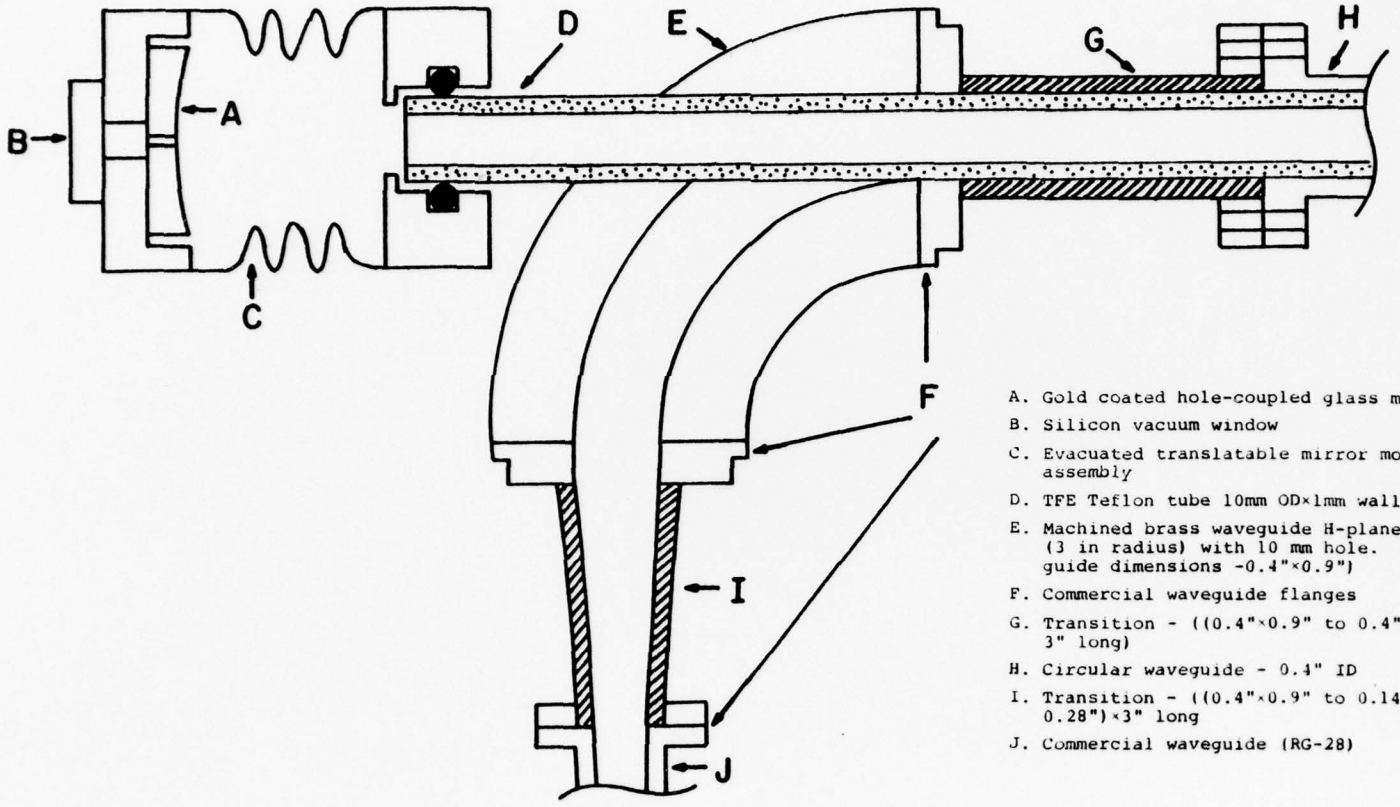

A. Gold coated hole-coupled glass mirror
B. Silicon vacuum window
C. Evacuated translatable mirror mount assembly
D. TFE Teflon tube 10mm OD×1mm wall
E. Machined brass waveguide H-plane bend (3 in radius) with 10 mm hole. (Waveguide dimensions -0.4"×0.9")
F. Commercial waveguide flanges
G. Transition - ((0.4"×0.9" to 0.4"ID)× 3" long)
H. Circular waveguide - 0.4" ID
I. Transition - ((0.4"×0.9" to 0.14"× 0.28")×3" long
J. Commercial waveguide (RG-28)

Figure 3. Resonator cell.

and the commercial 35 GHz waveguide is terminated with a matched load. In this configuration the cell is called the travelling wave cell. A short can replace the matched termination to produce a standing wave configuration.

The microwave circuit characteristics of the resonator cell exhibits strong dependence on microwave frequency. The measured VSWR was typically in the range of 1.8 to 3. For a given frequency, a stub tuner was used to reduce the VSWR to a 1.4 minimum value. The resulting structured microwave power transmission spectrum has a significant effect on the observed double resonance experiments as will be discussed later.

The infrared radiation is focused through the salt window and hole coupled gold coated glass mirror. The focal length of the focusing mirror is approximately equal to the length of the cell. The majority of the infrared radiation overlaps the modes of the FIR resonantor formed by the two hole coupled mirrors. The cell has been used without hole coupled mirrors to perform IMDR experiments.

The FIR resonator consists of two hole coupled mirrors and the 8 mm ID aperture dielectric (Teflon) tube. The separation and curvature of the mirrors form a stable open resonator. The dielectric tube may cause the FIR to operate in a waveguide mode.[7] This subject requires more attention and will be the subject of a future investigation.

Several points implemented in the cell design include:

1) The Teflon tubing was chosen because of its low loss at microwave frequencies. Polyflo (Eastman Kodak trademark) tubing may work but has not been tried. Quartz and Pyrex tubing have been used and rejected because of high-loss measured and ease of breakage.

2) The transitions were chosen to minimize the reflections from the Teflon tube and large aperture holes.

3) The Teflon tube and the two mirror mounts are the only components requiring evacuation.

4) A silicon vacuum window is used because of its broad-band FIR transmission characteristics.

The resonator cell offers the following features:

1) Collinear propagation of IR, FIR, and microwave radiations,

2) Feedback for the FIR,

3) Vacuum readily attainable. These three features are essential to success in producing infrared-microwave pumped FIR.

II-3 Molecular System

The choice of a suitable molecular system for infrared-microwave pumped SHRS is simplified by the reported infrared-microwave double resonance experiments. The work of Freund and Oka[8] in $^{14}NH_3$ has made the molecular system choice very direct.

The NH_3 inversion splittings, resulting from the nitrogen atom tunneling through the plane of the hydrogen atoms, produce a rich ground state microwave absorption spectrum. The fundamental ν_2 band leads to a rich infrared absorption band in the 10 micron range. These two features make ammonia a candidate for infrared microwave double resonance experiments. A detailed discussion of the molecular systems is given in the next section. The experiments will be performed with a CO_2 laser and a tunable 35 GHz magnetron in $^{14}NH_3$.

III. Infrared Microwave Double Resonance

Infrared-Microwave Double Resonance is a two-photon absorption experiment. This section will discuss: general two-photon theoretical results; application of results to $^{14}NH_3$, including selection rules; calculation of $^{14}NH_3$ two-photon transitions; two-photon absorption data acquisition techniques; and experimental results obtained.

III-1 Two-Photon Absorption

Two-photon absorption is a non-linear effect. An energy level diagram for two photon absorption is shown in Fig. 4.[8] The diagram depicts cases using infrared and microwave photons, ν_ℓ and ν_m, to make a transition from state 1 to state 3. All the states are assumed to have definite parity and transitions must be allowed from state 1 to state 2 and state 2 to state 3 (i.e., μ_p, $\mu_v \neq 0$). The transition

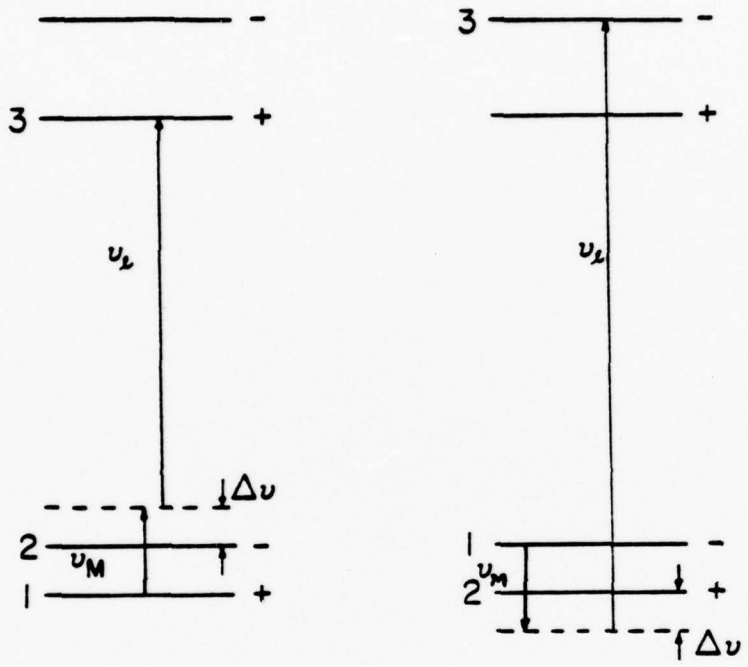

Figure 4. Two-photon absorption states of definite parity.[8]

probability for this process is given in Equation (3).

$$|M_2|^2 = \left| \frac{\langle 1|\bar{\mu}_p \cdot \bar{E}_m|2\rangle\langle 2|\bar{\mu}_v \cdot \bar{E}_\ell|3\rangle}{2h^2\Delta\nu} \right|^2 \qquad (3)$$

Equation (3) assumes the two-photon process is resonant (i.e., $\delta\nu = 0$ in Fig. 1). M_2 is called the "two-photon transition moment". The important points of Equation (3) indicate linear dependence of transition probability on laser and microwave powers and inverse quadratic behavior with respect to intermediate mismatch, $\Delta\nu$,

III-2 Two-Photon Absorption in NH_3

Fig. 4 shows the general case for two-photon absorption, and Equation (3) gives the transition probability. This section will describe application of NH_3 data to Equation (3) and Fig. 4.

The transition dipole moments, $\bar{\mu}_p$ and $\bar{\mu}_v$ are defined in Equation (4).

$$\bar{\mu}_i = |\mu_i| \; \bar{\Phi}_{JKM,J'K'M'}$$

$$\mu_i = \mu_p, \; \mu_v \qquad |\mu_p| = 1.468 \text{ debye}^{10} \qquad |\mu_v| = 0.25 \text{ debye}^{10} \qquad (4)$$

$\Phi_{JKM,J"K"M'}$ is the direction cosine matrix element. A more detailed discussion of this is given in Townes and

Schawlow,[9] and the corresponding formulae are given in Table 4-4 of Ref. 9.

The letters J,K,M,J',K', and M', are quantum numbers that identify the energy level states. In NH_3 states 1 and 2 are inversion split rotational energy levels in the ground state. State 3 is one of the inversion levels in the vibrationally excited ν_2 state. The spectroscopic notation used to describe the $^{14}NH_3$ energy levels is as follows:

LEVEL	PARITY	STATE
Gs(J,K,M)	+	Ground
Ga(J,K,M)	-	
ν_2s(J,K,M)	+	ν_2
ν_2a(J,K,M)	-	

J - total angular momentum quantum number.

K - ($\leq$ J) - projection of the total angular momentum on the molecular axis.

M - (= -J,.., O.., +J) - projection of the total angular momentum on a space fixed axis (i.e., laboratory reference frame).

The M quantum number is usually not specified because each of the M levels are degenerate in the absence of an external perturbing field.

The selection rules for single photon transitions in NH_3 are:

$\Delta J = J' - J = 0, \pm 1$

$\Delta K = K' - K = 0$, (± 3, perturbation allowed)

$\Delta M = M' - M = 0$

	$s \rightarrow a$	$a \rightarrow s$	
$\Delta v = 0, \pm 1$	0		pure rotation
	± 1		VIBRATION-ROTATION

The spectroscopic notation used identified the initial state and type of transition involved. P, Q, R transitions indicate ΔJ = -1. 0, +1, respectively. For all cases here only $\Delta K = 0$ transition will be considered. For a discussion of the $\Delta K = +3$ perturbation allowed transitions, see Ref. 8.

The Δv selection rule implies a pure rotation transition or a vibration rotation transition. The notation used to identify which process is involved is to specify the state for pure rotation transitions. Examples are:

NOTATION	INITIAL LEVEL	FINAL LEVEL
G:sP(J,K)	Gs(J,K)	Ga(J-1,K)
ν_2:aQ(J,K)	ν_2a(J,K)	ν_2s(J,K)
sR(J,K)	Gs(J,K)	ν_2a(J+1,K)

The two-photon selection rules for NH_3 are:

$\Delta J = 0, \pm 1, \pm 2$

$\Delta K = 0$

$\Delta M = 0, \pm 1$

$$a \rightarrow a \qquad s \rightarrow s$$

$$\Delta v = 0, \pm 1, \pm 2$$

The notation for the two photon transitions is similar but considerably more involved. Only the infrared-microwave cases will be considered at this time. The microwave frequencies will always be interacting with inversion transitions (Q type rotational) in the ground state. The two-photon selection rules then reduce to:

$$\Delta J = 0, \pm 1$$

$$\Delta K = 0$$

$$\Delta M = 0, \pm 1$$

$$a \rightarrow a \qquad s \rightarrow s$$

$$\Delta v = \pm 1$$

The allowed two-photon transitions considered here are identified in Table 1. The relative polarization indicates the orientation of the infrared with respect to the microwave. This assumes linear polarization of the infrared and microwave. The orientation listed under $\Delta M = 0$ is the preferred polarization, as is determined from the direction cosine matrix element. The frequency listed gives the most resonance enhanced frequency (i.e., $\Delta\nu$ is smaller if this condition is true). This is important because the intermediate mismatch $\Delta\nu$ is large to begin with for the systems under study.

Table 1. Infrared-microwave two-photon transitions considered in this investigation.

TRANSITION IDENTIFICATION	INITIAL LEVEL	INTERMEDIATE LEVEL	FINAL LEVEL	RELATIVE POLARIZATION ΔM=0	RELATIVE POLARIZATION ΔM=±1	FREQUENCY
sQP(J,K)	Gs(J,K)	Ga(J,K)	ν_2s(J-1,K)	⊥	||	$\nu_\ell+\nu_m$
aQP(J,K)	Ga(J,K)	Gs(J,K)	ν_2a(J-1,K)	⊥	||	$\nu_\ell-\nu_m$
sQQ(J,K)	Gs(J,K)	Ga(J,K)	ν_2s(J,K)	||	⊥	$\nu_\ell+\nu_m$
aQQ(J,K)	Ga(J,K)	Gs(J,K)	ν_2a(J,K)	||	⊥	$\nu_\ell-\nu_m$
sQR(J,K)	Gs(J,K)	Ga(J,K)	ν_2s(J+1,K)	⊥	||	$\nu_\ell+\nu_m$
aQR(J,K)	Ga(J,K)	Gs(J,K)	ν_2a(J+1,K)	⊥	||	$\nu_\ell-\nu_m$

This completes the infrared-microwave double resonance selection rules and spectroscopic notation discussion. Calculation of IMDR frequencies are now possible.

III-3 Infrared-microwave Double Resonance Frequencies in $^{14}NH_3$

The calculation of two-photon transition frequencies was accomplished by taking the difference between the final state and initial states defined by the selection rules of the previous section. The energy levels listed in a Ph.D. thesis by J. Curtis,[11] have been used for the calculation. These energy levels have been compiled and reorganized in Malk's M.S. thesis.[12]

The transition frequencies were sorted in ascending order and merged with the previously calculated CO_2 laser frequencies.[10] The result is a list of two-photon absorption frequencies and CO_2 laser frequencies in ascending order. Taking the difference/sum between/of CO_2 laser and two-photon transition frequencies yields the required microwave frequency for a double resonance condition.

The microwave frequency range of interest is from 33 to 35 GHz. This further restriction filters many of the possible matches, until nine candidate systems are found. The resulting molecular systems are listed in Table 2.

Table 2 also contains information regarding competing linear absorption of the infrared photons, the experimentally

Table 2. $^{14}NH_3$ double resonance systems.

CO_2 LASER TRANSITION FREQUENCY (CM^{-1})	NH_3 TWO PHOTON TRANSITION FREQUENCY (CM^{-1})	MICROWAVE* FREQUENCY (GHz)	NH_3 LINEAR COMPETITION FREQUENCY (CM^{-1})	PROBABLE EMISSION TRANSITION FREQUENCY (CM^{-1})
$P(38)_{10}$	sQQ(6,6)			aP(7,7)
927.0083234	928.1576	34.4783 M (34.501) O		788.5064
$P(34)_{10}$	sQQ(2,2)	33.6950 M		aP(3,2)
931.0014322	932.1246	(33.674) O		871.7371
$P(24)_{10}$	sQQ(11,4)		2sQ(7,5)	ν_2:aR(10,4)
940.5480971	941.6504	33.0691	940.4806	193.8715
	sQQ(12,5)			ν_2:aR(11,5)
	941.6706	33.6751		213.9626
$P(20)_{10}$	sQQ(12,2)		2sQ(4,2)	ν_2:aR(11,2)
944.1940288	945.3138	33.5931	944.1425	251.3279
$R(16)_{10}$	aQQ(6,3)		sQ(5,4)	ν_2:sR(5,3)
966.2503603	965.1289	33.6438	966.2684	150.8906
$R(9)_{10}$	aQQ(3,3)		sQ(2,2),sQ(2,1)	ν_2:sQ(3,3)
967.7072329	966.5524	34.6450 M (34.677) O	967.7492	35.7914
$P(40)_9$	aQR(2,2)			ν_2:sR(2,2)
1027.3821707	1026.2442	34.1391 M		94.9109
	aQR(2,1)			ν_2:sR(2,1)
	1026.2805	33.0501 M		94.1452

*O - EXPERIMENTALLY OBSERVED BY FREUND AND OKA, PHYS. REV. A, 13(6), 2178 (1976).
M - EXPERIMENTALLY OBSERVED BY MALK.

observed microwave frequencies of Freund,[8] and the most probable transition for emission as a result of the two-photon pumping and its frequency. The other experimentally observed double resonances have been accomplished by Malk and are the subject of this report. The frequencies listed in Table 2 are all theoretical with the exception of those observed by Freund in parentheses.

An interesting feature of the experimentally observed double resonance is the difference in the J and K quantum numbers. For J equal K the direction cosine matrix element is at maximum value for the inversion transitions. The direction cosine matrix element is always less than or equal to 1, and is a quadratic term in the numerator of Equation (3). Hence for J equal K the maximum double-resonance signal is observed.

III-4 Experimental Apparatus and Data Acquisition

Two types of Infrared Microwave Double Resonance (IMDR) experiments have been performed. The microwave pumping source used determines the type of experiment. A CW Elliott Brothers B579 Klystron and a pulsed SFD 330 tunable magnetron have been used. The data acquisition techniques developed for the experiments will also be detailed.

III-4.1 Reported IMDR Experimental Techniques

The design of an experiment to produce tunable FIR using SHRS is not optimal for performing IMDR experiments.

The usual IMDR experiment[8,5] consists of a cell containing the gas of interest through which the microwaves and infrared are co-propagated. The microwaves are usually frequency modulated with a square wave while the microwave center frequency is slowly changed. A double-resonance signal appears when the square wave modulation is detected on the transmitted infrared signal. The modulated infrared signal is easily detected using phase-sensitive detection (PSD) techniques and usually produces a signal derivative with respect to frequency. Tremendous improvement of the observed signal-to-noise ratios are achieved by insertion of the cell into the infrared laser cavity.[5] This kind of experiment produces high quality spectroscopic data. The IMDR technique allows for measurement of infrared transition frequencies with microwave frequency measurement accuracy.

The experiments to be described are intended as an intermediate step in the generation of FIR, and therefore are more concerned with the amount and linewidth of two-photon absorption rather than the absolute frequency of the infrared transition.

III-4.2 CW IMDR Experiment

The CW IMDR experiment was performed with a fixed frequency Elliott Brothers Klystron. Only one molecular system could be studied because of the non-tunablility of the Klystron. The experimental apparatus is shown in Fig. 5.

The CO_2 laser is approximately 1 meter long, with KCl Brewster windows. The optics for the laser consist of a 10

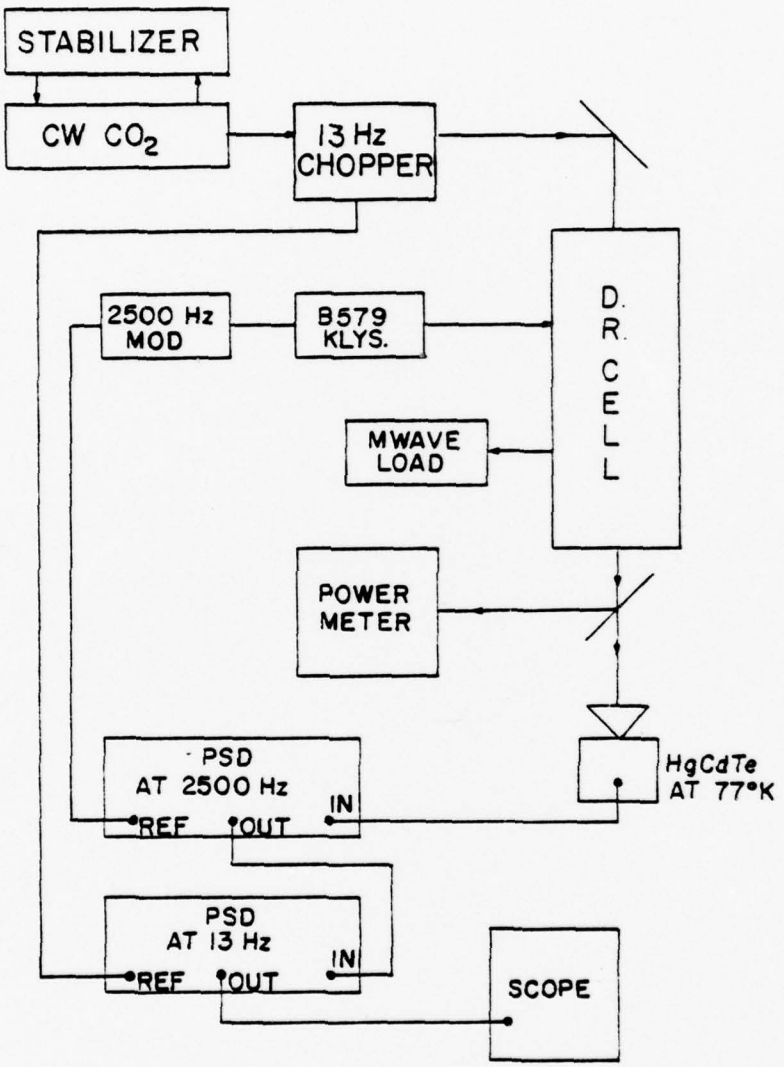

Figure 5. CW double resonance experiment.

meter radius of curvature PTR master grating, blazed at 10.6 microns, ruled in Si and gold plated, and an 80% Ge partial reflector. The cavity is dither stabilized using a Lansing stabilizer and PZT with a pyroelectric detector used in the feedback loop. The laser operated at 1½ watts on the R(8) 10 micron transition of CO_2 with a flowing gas mix, 1:2:4 (CO_2:N_2:He), at a pressure of 20 torr. The output of the laser was amplitude modulated by a 13 Hz mechanical chopper. The laser radiation is passed through the waveguide double resonance cell (see section II.1), and is split by a silicon beam splitter. Part of the beam is monitored with a Scientech Power meter and the rest is incident on the HgCdTe (@77°K) detector.

The microwave source, a B579 Klystron, 9.3 watts at 36.68 GHz, is passed through an isolator and tuning stub into the cell. After the cell a 30 db coupler in connection with an 1N53 diode are used to monitor the transmitted microwave power. The remaining microwave power is dissipated in a high power forced-air cooled dummy load. The microwave radiation is amplitude modulated (M=0.14) at 2500 Hz. The tube is also being frequency modulated to an unknown degree. This was observed by beating the amplitude modulated B579 Klystron with a CW OKI 35V10 Klystron in a 1N53 diode. A periodic chirp was observed while amplitude modulation was applied. The magnitude of the frequency chirp was not measured.

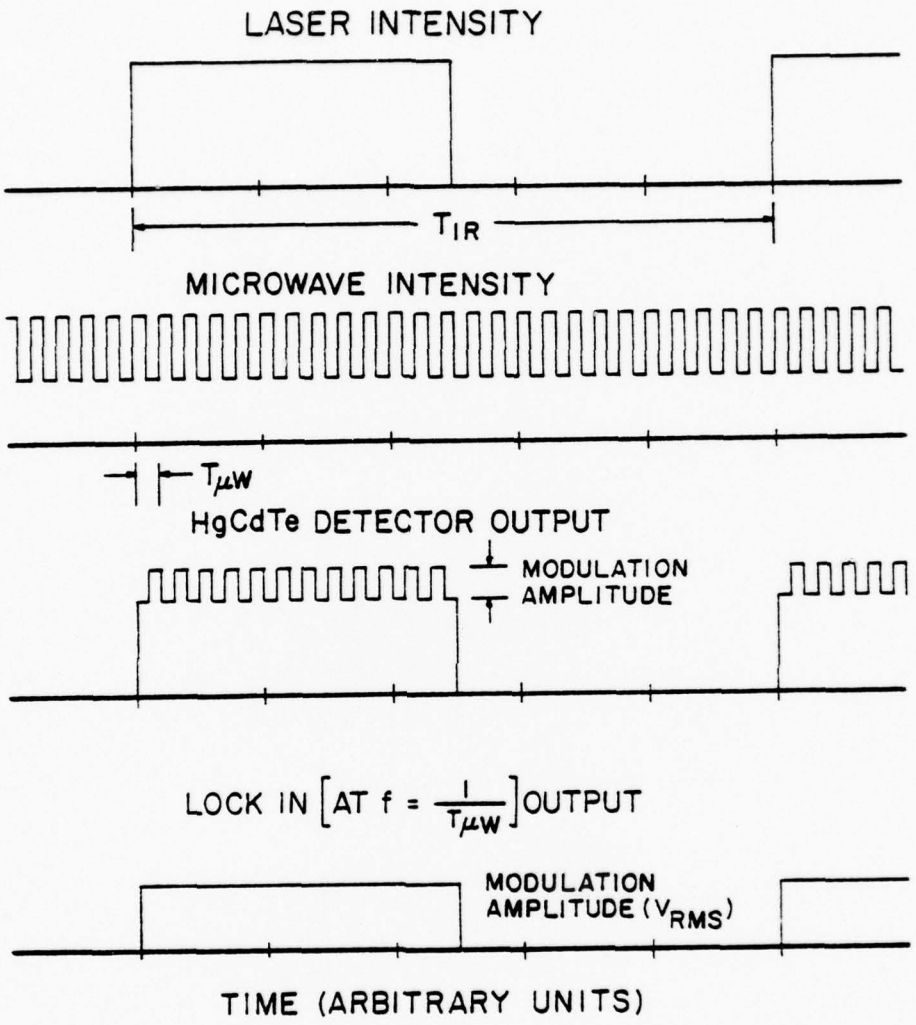

Figure 6. CW two-photon absorption detection technique.

The detection equipment used consists of the HgCdTe detector, two lock-in amplifiers (PAR-HR8) and an oscilloscope or chart recorder.

The two-photon absorption detection technique is shown in Fig. 6. The time scale shown is arbitrary, as is the relative phase between the infrared and microwave intensities. The laser intensity is amplitude modulated with a 50% duty cycle at $f_{IR}(=1/T_{IR})$Hz. The microwave intensity is modulated similarly at $f_{\mu\omega}(=1/T_{\mu\omega})$Hz. The modulation index of the microwave is shown to be less than 1, which is the experimentally observed case for the Elliott Brothers Klystron. If two-photon absorption occurs then modulation at $f_{\mu\omega}$ will be observed on the infrared signal. Phase sensitive detection (PSD) at $f_{\mu\omega}$ is used to detect the RMS amplitude of this modulation. If the double resonance signal is sufficiently large, the output of the lock-in amplifier may be observed directly on an oscilloscope. The sensitivity can be greatly increased by connection of the mixer output of the PSD to a second lock-in amplifier at f_{IR}. Care must be taken to avoid saturating the input of the second lock-in amplifier. This is essential to obtaining meaningful data. The technique described is a double modulation technique.

The apparatus and detection technique described have been used to obtain CW infrared-microwave double-resonance data. The data will be discussed in the Experimental Results section of this report.

III-4.3 Pulsed IMDR Experiment

The pulsed experiment was performed with a tunable SFD 330 magnetron and a CW CO_2 laser. The tunable feature of the magnetron adds tremendous flexibility to the choice of a suitable molecular system. The experimental apparatus is shown in Fig. 7.

The CO_2 laser, chopper, detector, and power meter have already been described in the previous section. For the pulsed experiment, the pumping source and double resonance cell are changed.

The SFD-330 magnetron is rated at 30-40 kwatts in the 33.5 to 35.5 GHz frequency range. The achieved power is approximately 30 kwatts in the 33.0 to 35.0 GHz range. The spectral purity of the magnetron is unknown. The magnetron is operated in a pulsed mode at 300-400 Hz repetition rate with a 1 μsec pulse width. The power is sufficiently strong to "break down" the inside of the waveguide with a VSWR greater than 2.0. The remainder of the microwave circuit is essentially the same as before, with the exception of the transmitted power monitor branch. An addition of 40 db of variable attenuation is added before the 1N53 diode to prevent destruction of the diode.

Two cells have been used to perform the double resonance experiments. The waveguide double resonance cell and the resonator cell, without the FIR feedback mirrors, have produced results that will be described in detail.

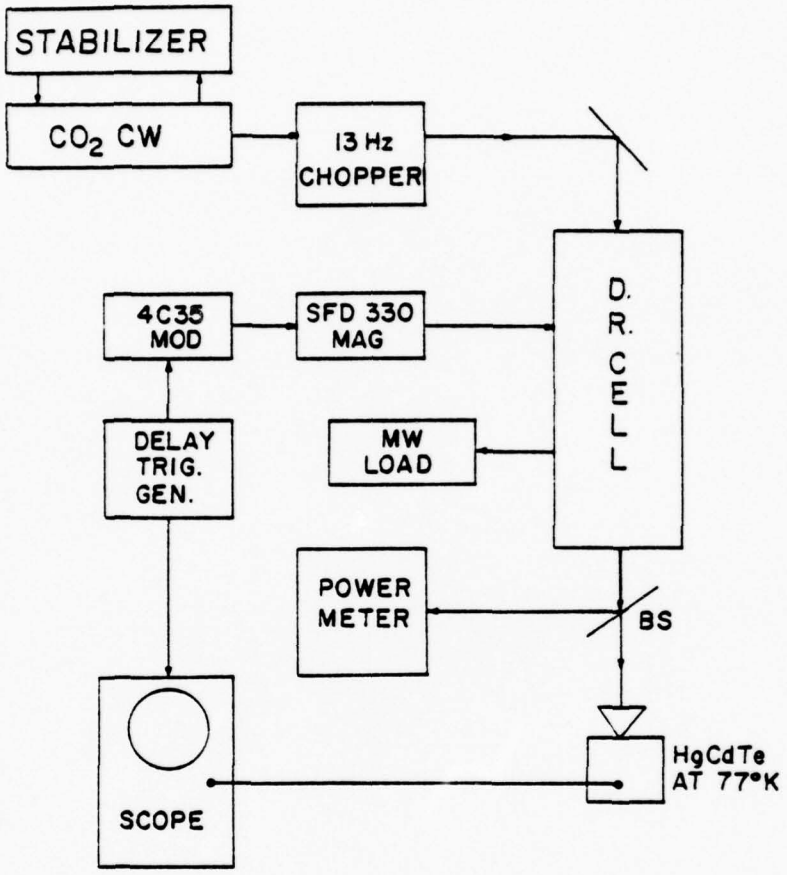

Figure 7. Pulsed double resonance apparatus.

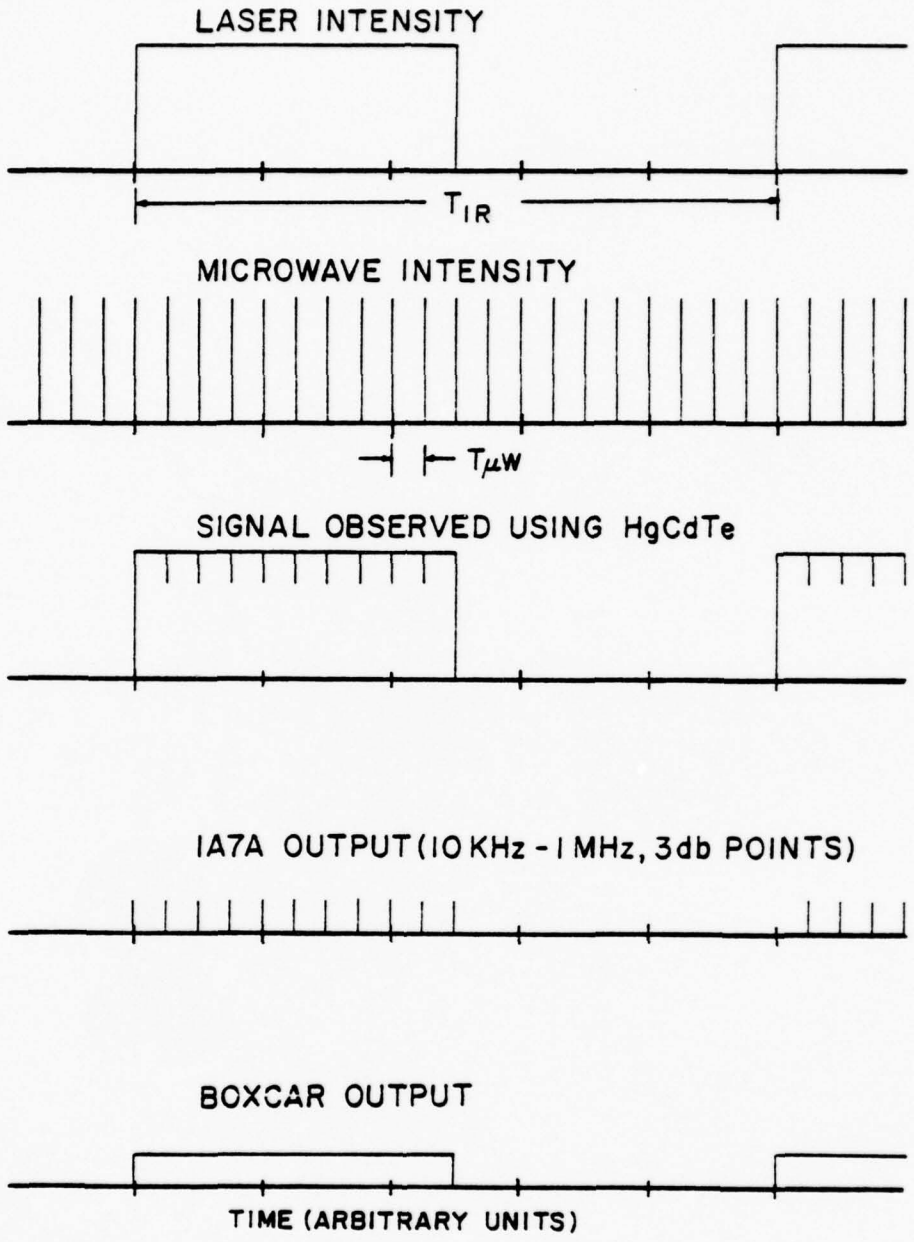

Figure 8. Pulsed two-photon absorption detection technique.

The detection technique employed for the pulsed experiments are different than the technique previously described. The low duty cycle ($\cong$ 0.0007) of the microwave makes PSD at the microwave repetition rate frequency less sensitive. The observed double resonance signals using the magnetron have been easily observed using direct detection. A technique for detection of much smaller signals has been realized.

The detection scheme is shown in Fig. 8. The laser intensity is modulated at $f_{IR}(= 1/T_{IR})$. The microwave pulses occur at a $f_{\mu\omega}$ repetition rate. The pulse width, τ, of the magnetron now becomes important in choosing an appropriate high-pass filter. The signal observed on the HgCdTe detector has frequency components at $f_{\mu\omega}$, f_{IR}, and $f_p(\cong 1/\tau)$. In the cases considered, $f_p >> f_{\mu\omega}$, f_{IR}. The filter is chosen to pass f_p and reject f_{IR} and $f_{\mu\omega}$. The components at $f_{\mu\omega}$ are very small and can be ignored. The Tektronix 1A7A high gain differential amplifier is ideal for this purpose, since it features a variable band pass filter on the input stage. The low frequency components of the detector signal are filtered out, and a series of pulses are observed when the laser intensity is present. The inverted 1A7A output is shown in the figure. All the signals observed to date have detected in this manner.

A double modulation detection scheme is easily implemented with the use of a gated high-speed sample and hold circuit and a lock-in amplifier. A Boxcar integrator has been used as the

high-speed sample and hold circuit. The output of the band pass filter is stored in the sample and hold and reset every microwave pulse. The sample and hold effectively stretches the duty cycle of the microwave modulation to 100%. The output of the sample and hold will appear to be a square wave at f_{IR}, and can be detected using PSD. Again, care must be taken to avoid saturating any of the amplifiers in the chain if meaningful results are to be achieved.

The development of the double modulation techniques described and the design of these experiments is hoped to provide the essential experience required to produce tunable far infrared generation.

III-5 Experimental Results

Infrared microwave double resonance experiments have been performed using four different CO_2 laser transitions in $^{14}NH_3$. The CO_2 $R(8)_{10}$ + 34.68 GHz resonance with the aQQ(3,3) two-photon transition has been investigated in more detail than the other systems. Only the $R(8)_{10}$ experiments will be detailed here. The pertinent data of the other experiments is contained in Table 2 of Section III-3.

III-5.1 CO_2 $R(8)_{10}$ Molecular System in $^{14}NH_3$

The decision to study this system was reached for several reasons. The Gs(3,3) and Ga(3,3) energy levels have the greatest partitioning of population at room temperature. This two-photon transition has been observed by Freund[8] and

accurate frequency measurements have been obtained for the infrared transition. The microwave inversion transition has been studied and the linewidth measured. An energy level diagram relevant to the CO_2 $R(8)_{10}$ transition is depicted in Fig. 9.

The two-photon transition is the aQQ(3,3) transition. A microwave frequency of 34.677 GHz[8] less the CO_2 $R(8)_{10}$ transition at 967.707329 produce two-photon resonance. The intermediate mismatch for the two-photon process is 10.807 GHz. If two-photon pumping occurs one expect emission on the ν_2:sQ (3,3) transition at 35.79 cm^{-1} ($\lambda \cong 279$ μm). A competing linear infrared absorption occurs on the sQ(2,2) transition, with a resonance mismatch of 940.2 MHz.[8] The Doppler width of a two-photon transition in $^{14}NH_3$ at 10 microns is 80 MHz and a homogeneous broadening rate of $\sim$ 30 MHz/torr. This indicates the two-photon transition should be Doppler broadened at pressures below 2 torr.

III-5.2 CW Results

The CW results were obtained with a CW CO_2 laser operating on the $R(8)_{10}$ transition and the B579 Klystron operating at 34.68 GHz. Fig. 10 shows a pressure scan of the signal in the waveguide double resonance cell with an interaction length of 1.5 meters. The two-photon absorption signal is defined as $\Delta I/I_o$ in Equation (5)

$$\frac{\Delta I}{I_o} = \frac{I_o - I_+}{I_o} \times 100$$

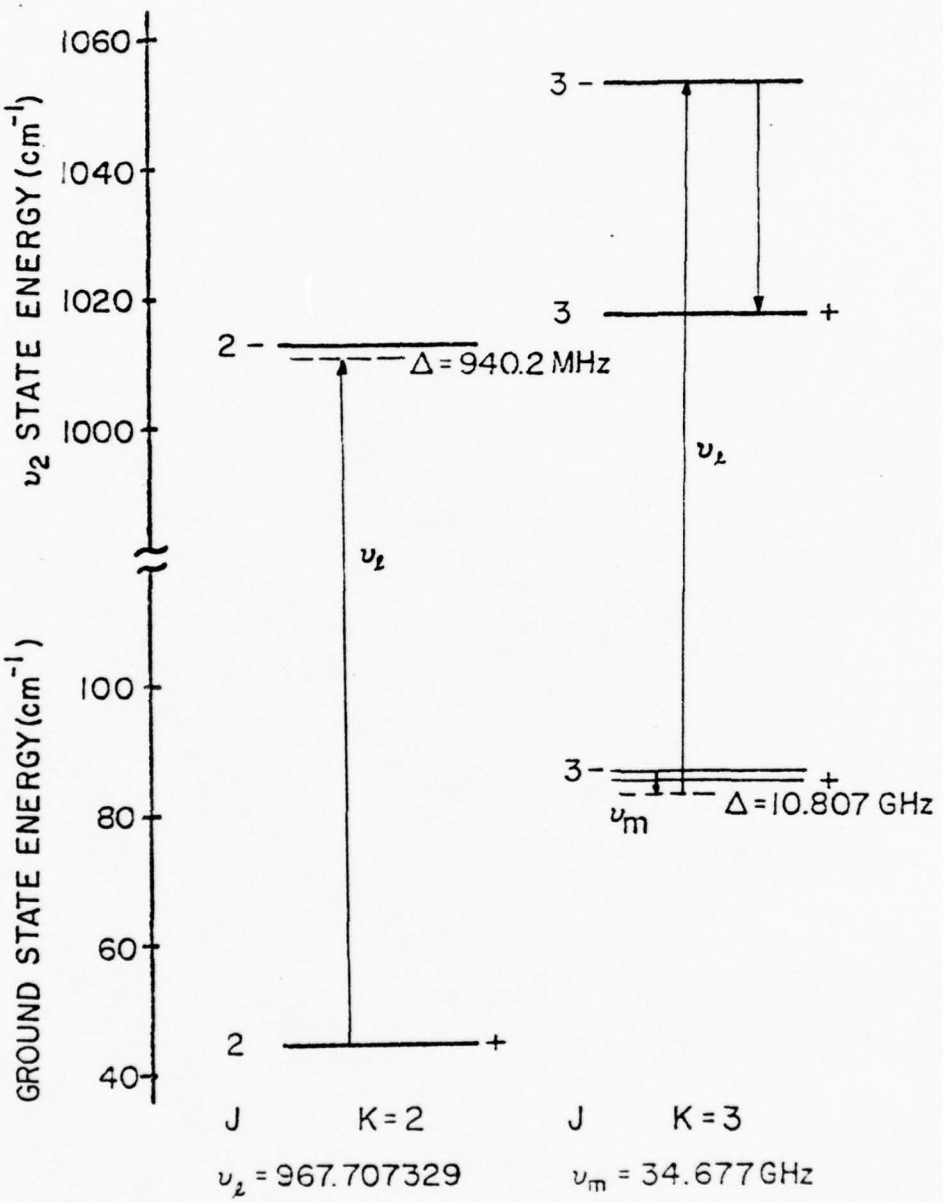

Figure 9. $^{14}NH_3$ energy levels relevant to $CO_2R(8)_{10}$.

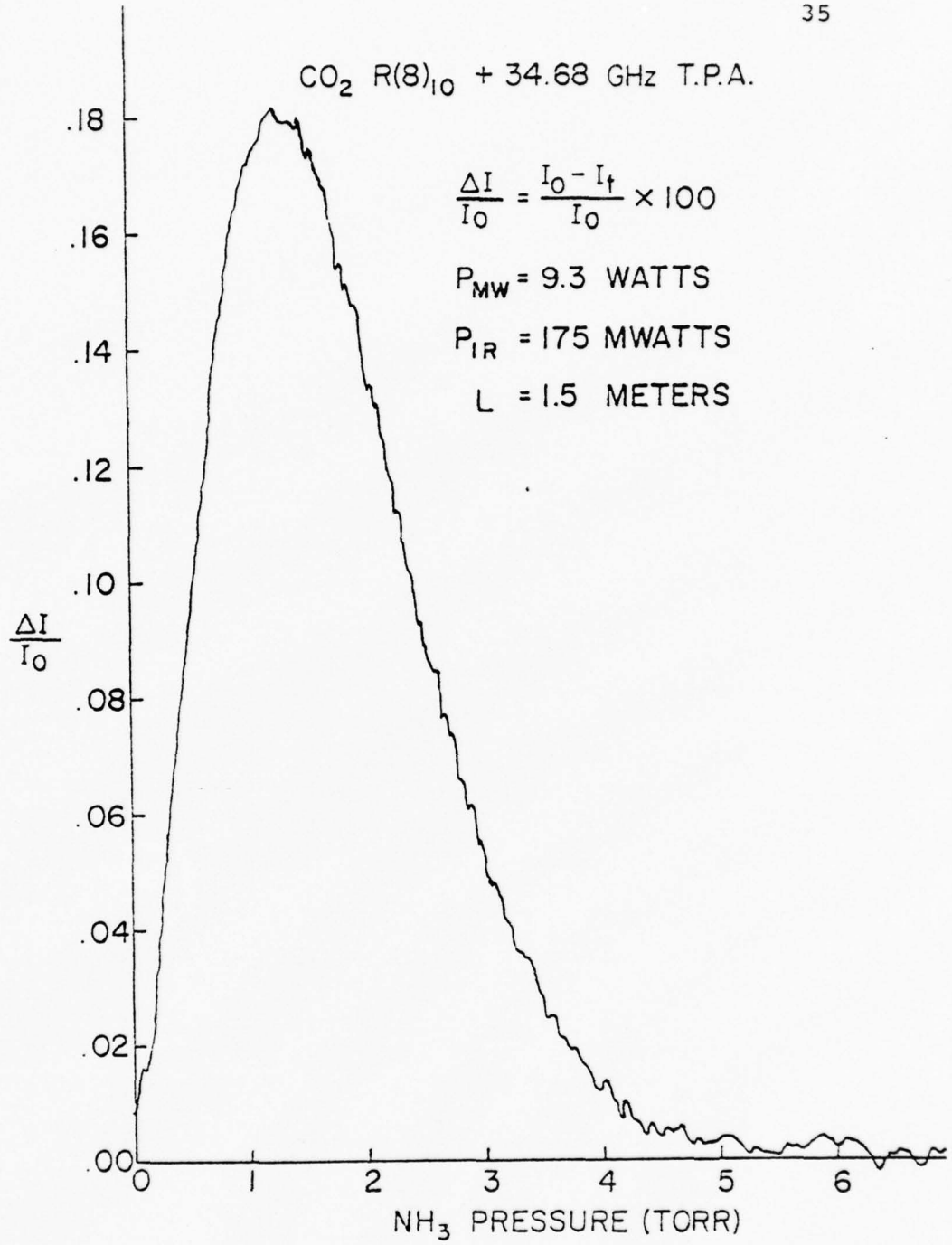

Figure 10. Two-photon absorption vs. pressure for CO_2 R(8)$_{10}$ + 34.68 GHz.

ΔI is the RMS amplitude of the microwave modulation frequency observed on the infrared signal with the HgCdTe detector. I_o is the zero pressure transmitted RMS power of the infrared, I_+ is the transmitted RMS power when two-photon absorption occurs. The signal was detected using the CW double modulation technique.

The significant features of Fig. 10 are the linear rise in signal at pressures less than 1 torr, the peak signal pressure, and the magnitude of the signals observed. The linear rise in the signal at pressures less than one torr indicates the two-photon transition is Doppler broadened. The magnitude of the two-photon absorption measured represent a maximum of 0.18 percent modulation of the infrared source, and indicate 0.02 percent modulation is detectable with a reasonable signal-to-noise ratio using the double modulation detection technique.

The peak pressure point deserves further consideration. It suggests that saturation of the infrared or microwaves has occurred; alternatively, the competing linear process may be depleting the infrared signal. Fig. 11 is an investigation of the possiblility of saturating the infrared radiation. The two-photon absorption is measured as the input infrared power is varied. The two lines were accomplished at different pressures. The line P = 1.2 torr corresponds to the peak signal pressure. In both cases the magnitude of absorption dependence is linear with infrared power. This is expected from

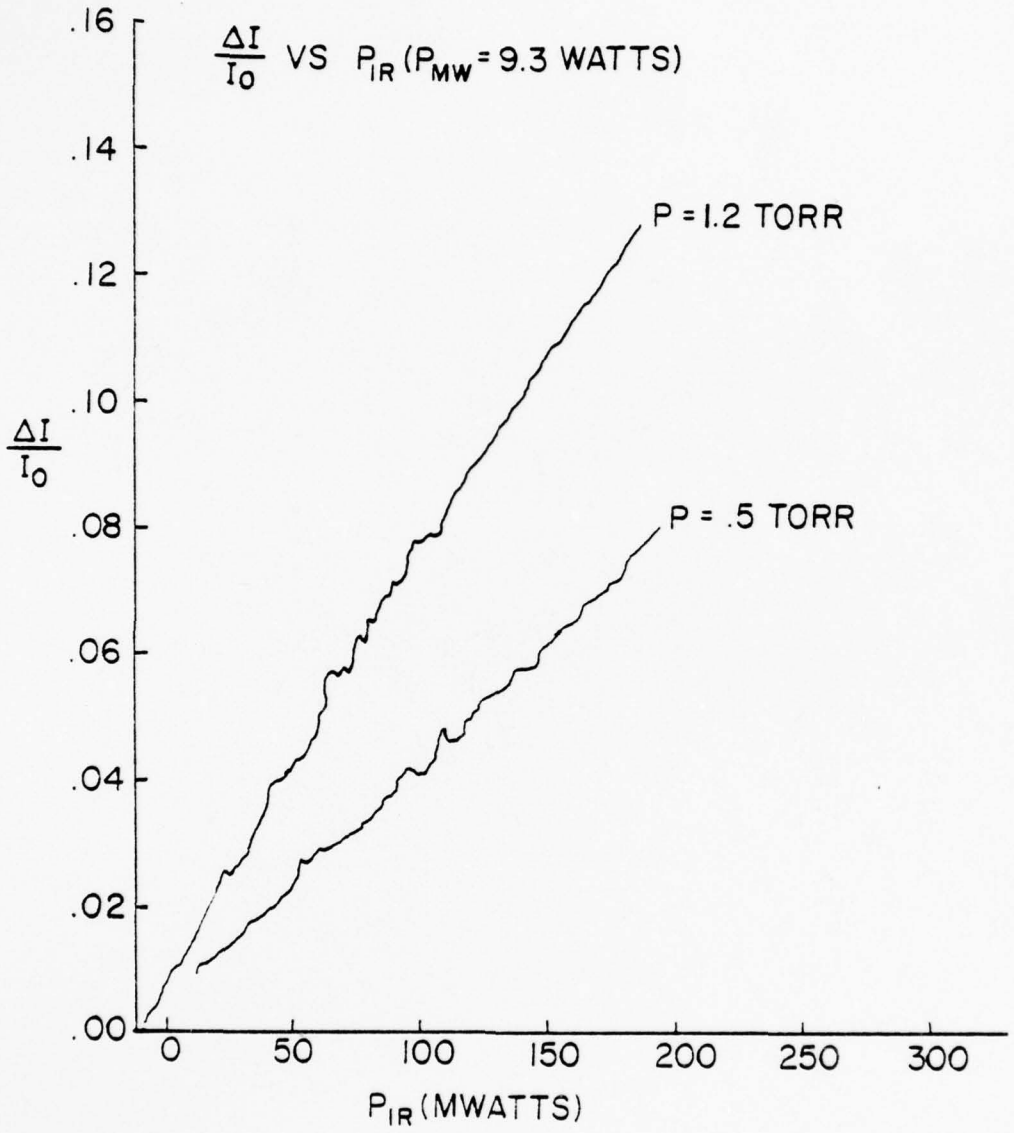

Figure 11. Two-photon absorption versus infrared laser power. P = 1.2 torr corresponds to peak absorption signal. P = 0.5 torr corresponds to Doppler broadened case (see Fig. 10).

Equation (3). This also rules out saturation of the infrared power. The transmitted infrared power was measured to be approximately 30% of the zero pressure transmitted power at the peak pressure of the two-photon signal. This partially explains the peak pressure.

The results observed for the CW experiments agree qualitatively with theory. A comparison of calculated and measured values show differences of 200-300%. A more detailed comparison will be performed at a later time.

III-5.3 Pulsed Results

The pulsed experiments were performed with a CW CO_2 laser and a tunable pulsed magnetron. The results here show larger amounts of two-photon absorption than have ever been reported before for this molecular system. Use of higher power microwaves is the reason for this stronger interaction.

Fig. 12 shows a curve similar to that reported in the CW section. The cell has been reduced in length to 0.64 meters. The observed maximum modulation is now up to 40%. A number that is forty times larger than theoretically predicted value. The peak pressure has also increased to almost 4 torr. Fig. 13 shows the effect of the competing linear absorption of the CO_2 $R(8)_{10}$ photons. The peak pressure now occurs when the CO_2 power is about 50% of the zero pressure power.

The results discussed thus far have not exploited the tunability of the microwave source. Fig. 14 contains two

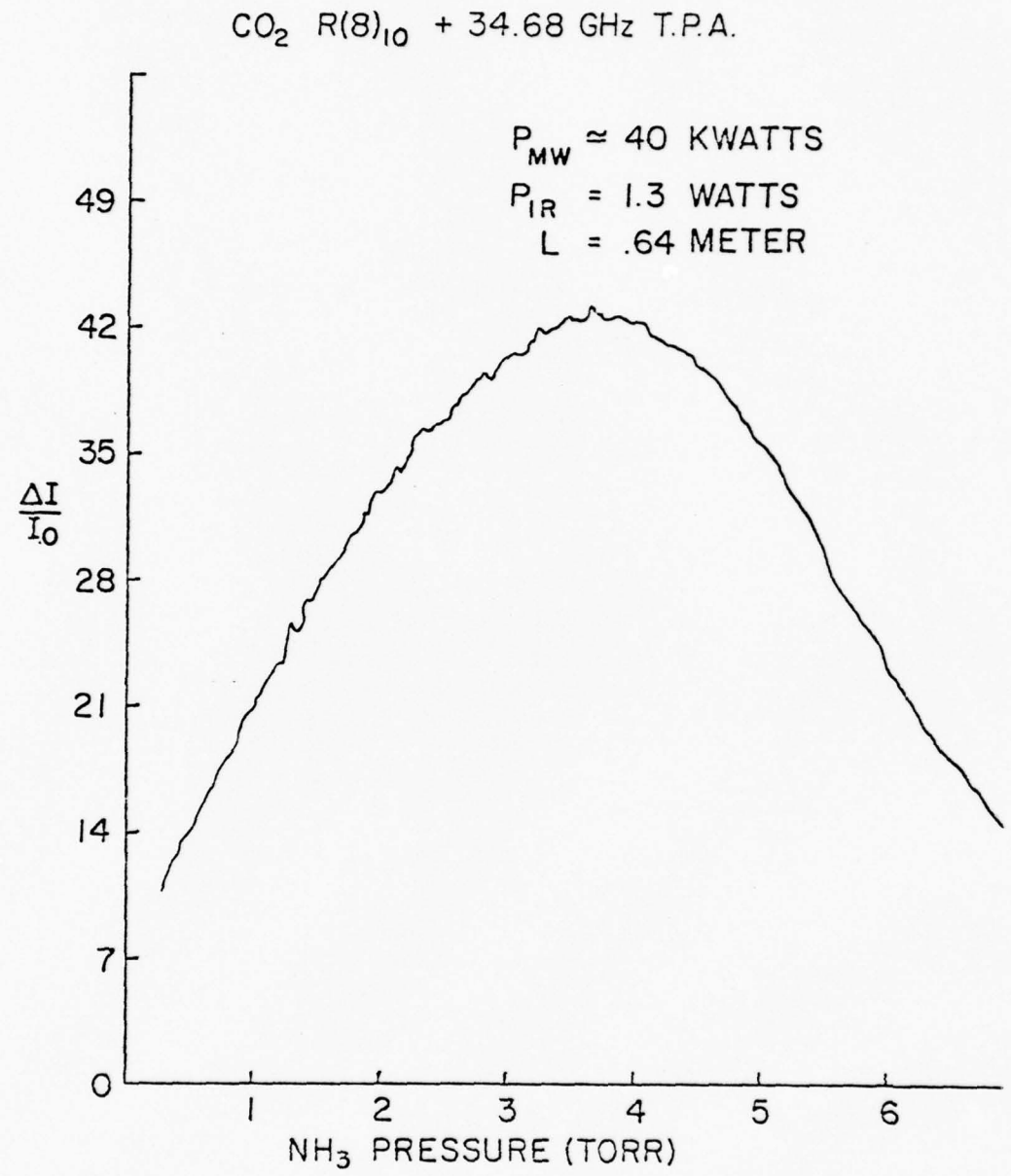

Figure 12. Pulsed two-photon absorption vs. cell pressure.

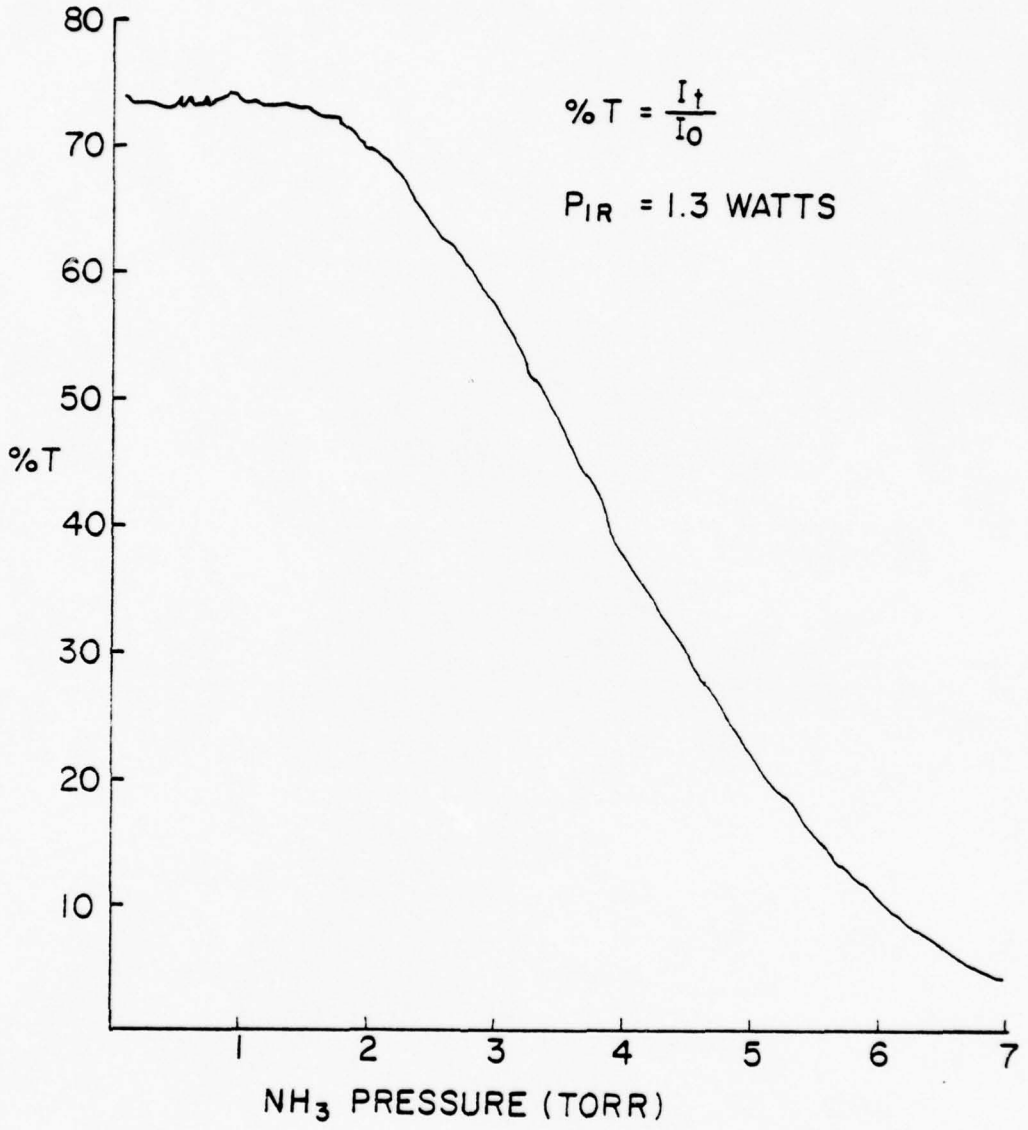

Figure 13. $CO_2R(8)_{10}$ transmission vs. NH_3 pressure.

curves. The upper curve is the transmitted microwave power as a function of magnetron frequency. The dips at 34.34 and 34.7 GHz represent unstable oscillation of the magnetron. The cell used for this graph is the waveguide cell (0.64m) and the cell pressure is 0.5 torr. The lower curve is the two-photon absorption curve. The curve is observed to be very broad in frequency range. The Doppler width of the transition is about 80 MHz, the observed width is significantly greater than this value. The structure of the two-photon curve is attributed to the variation of the transmitted microwave power.

Fig. 15 shows a similar set of curves for the resonator cell. The observed two-photon absorption is highly structured and similar in magnitude to the the results achieved in the waveguide cell. The structure is attributed to the microwave power transmission spectrum of the resonator cell.

The pulsed experiments produce IMDR signals with peak infrared modulations in excess of 40% of the zero pressure power. The signals exhibit broadening greater than the Doppler width of the two-photon transition. These results indicate that FIR generation using infrared-microwave optical pumping is feasible.

IV. Conclusions

A qualitative discussion of tunable FIR generation using infrared microwave pumped SHRS has been presented. Experimental

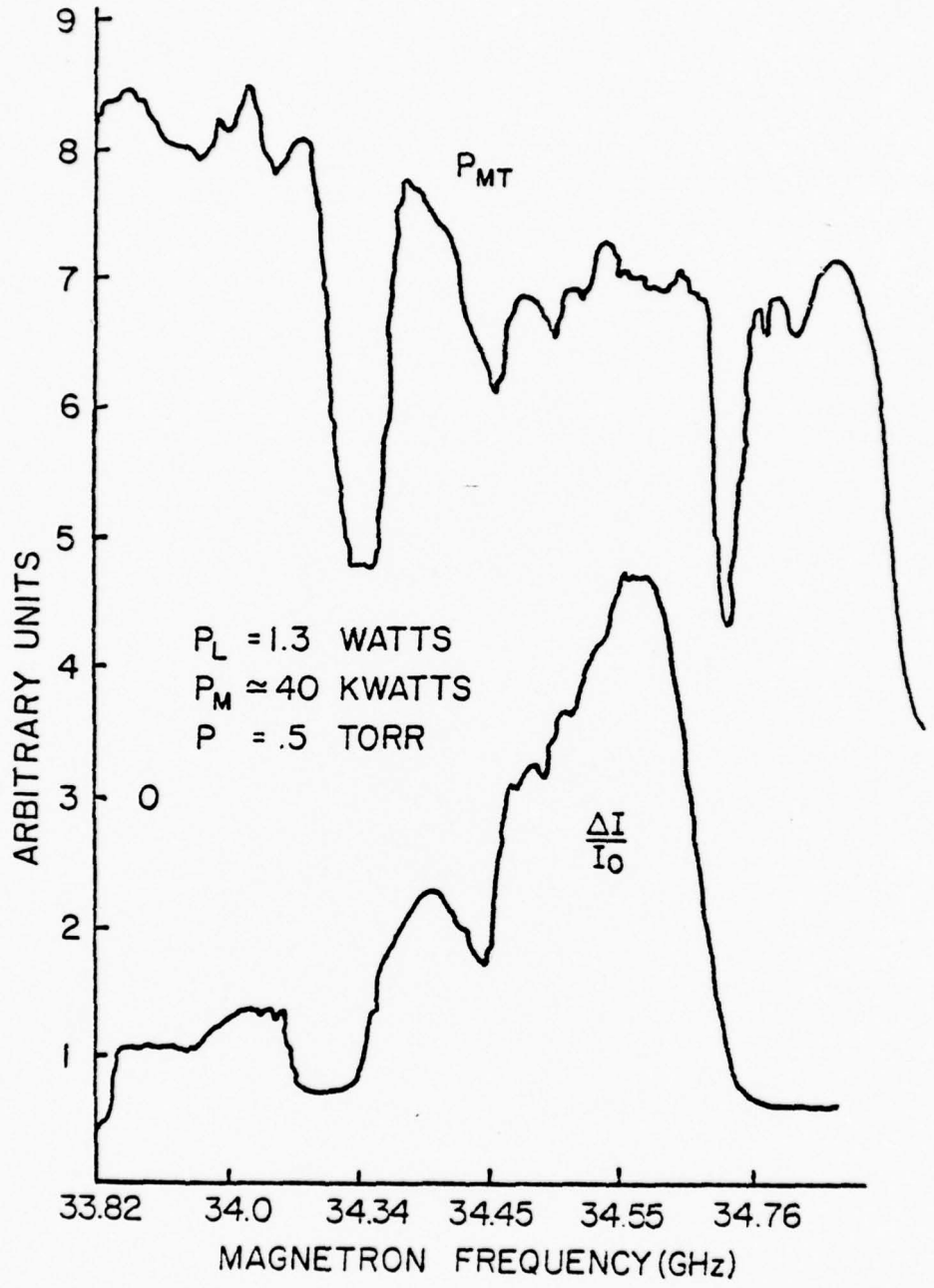

Figure 14. TPA and transmitted microwave power vs. frequency (waveguide cell).

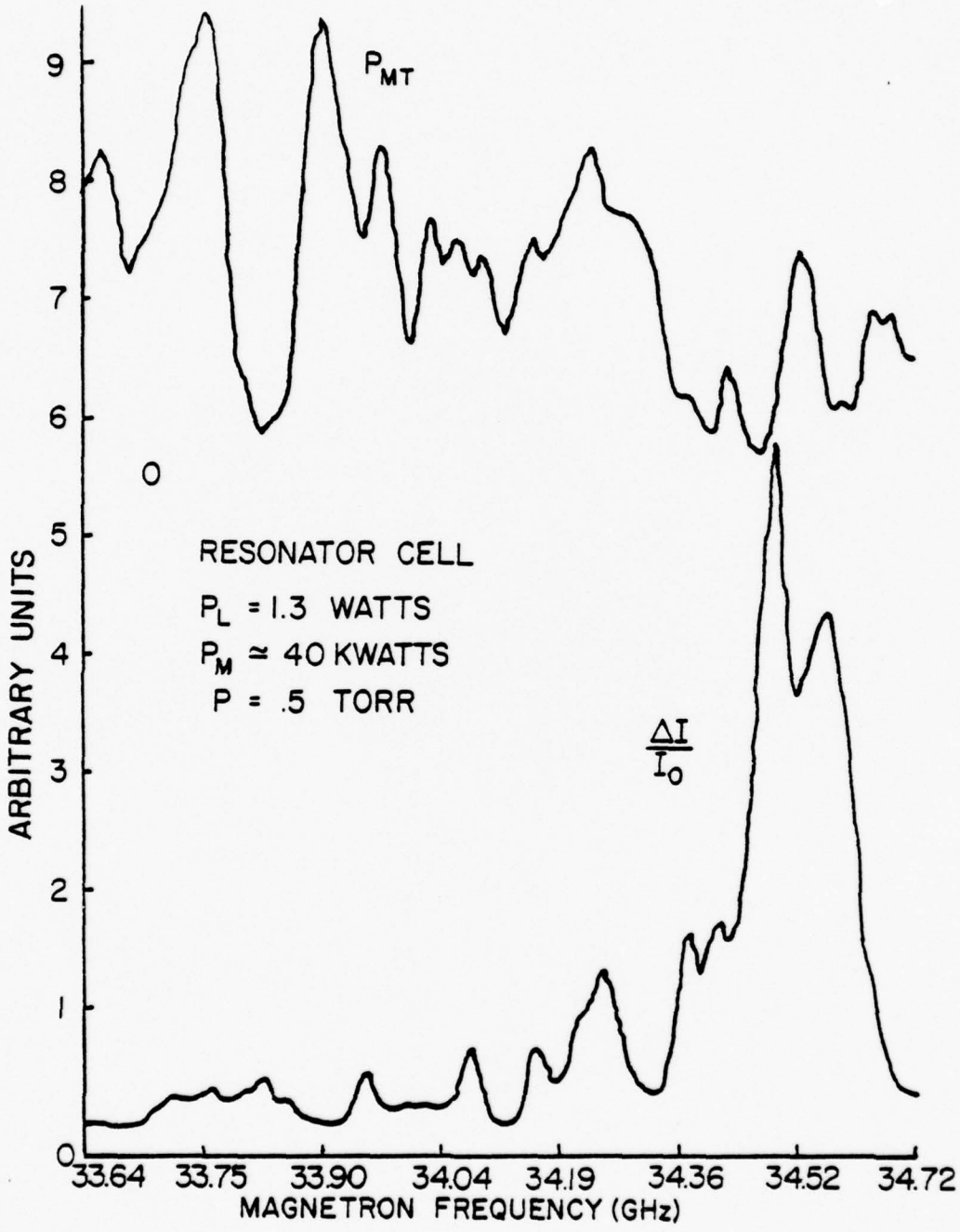

Figure 15. TPA and transmitted microwave power vs. frequency (resonator cell).

realization of this is currently under investigation. Preliminary results indicate that infrared-microwave optical pumping to generate FIR radiation is highly feasible. Significant pumping of the NH_3 molecule is indicated by the large modulation percentages of the infrared radiation caused by the two-photon absorption. The broad width of the two-photon absorption with respect to microwave pumping frequency suggests tunability of the FIR is a reasonable expectation.

The experimental realization of infrared-microwave pumped Stimulated Hyper-Raman Scattering will be a topic in the next report.

References

1. T. Y. Chang and J. D. McGee, "Off-resonant Infrared Laser Action in NH_3 and C_2H_4 without Population Inversion", Appl. Phys. Lett. 29(11), 725 (1976).

2. E. J. Danielewicz, E. G. Malk and P. D. Coleman, "High Power Vibration-Rotation Emission from $^{14}NH_3$ Optically Pumped Off-Resonance", Appl. Phys. Lett. 29, 557 (1976).

3. S. J. Petuchowski, A. T. Rosenberger and T. A. DeTemple, "Stimulated Raman Emission in Infrared Excited Gases", IEEE J. Quant. Elec. QE-13, 476 (1977).

4. D. Cotter, D. C. Hanna, W.H.W. Tuttlebee, and M. A. Yuratich, "Stimulated Hyper-Raman Emission from Sodium Vapor", Opt. Comm. 22, 190 (1977).

5. K. J. Kim and P. D. Coleman, to be published.

6. H. Jones, "Wide-band Intracavity Microwave Cells for Laser Microwave Double Resonance Spectroscopy", Appl. Phys. 14, 169 (1977).

7. E. J. Danielewicz, "Far Infrared Guided Wave Optics Experiments Using a Waveguide Laser with a Hybrid Output Mirror", Ph.D. Thesis, University of Illinois, Urbana, Illinois, 1976.

8. S. M. Freund and T. Oka, "Infrared-Microwave Two-photon Spectroscopy: The ν_2 Band of NH_3", Phys. Rev. A, 13(6), 2178 (1976).

9. C. H. Townes and A. L. Schawlow, Microwave Spectroscopy, (McGraw-Hill, New York, 1955).

10. a) W. K. Bischel, P. J. Kelly, C. K. Rhodes, "High-resolution Doppler-free Two-photon Spectroscopic Studies of Molecules. II. The ν_2 Bands of $^{14}NH_3$ Phys. Rev. A, 13, 1829 (1976).
    b) W. K. Bischel, "Application of Nonlinear Optical Techniques for the Investigation of Molecular Properties and Collisional Processes", Ph.D. Thesis, University of California, Livermore, CA (1975).

11. J. Curtis, "Vibration-Rotation Bands of NH_3 in the Region 670 cm^{-1}-1860 cm^{-1}", Ph.D. Dissertation, The Ohio State University, 1974.

12. E. G. Malk, "Superfluorescent Emission at 12.08 Microns and Off-resonant Emission at 11.46 Microns in Ammonia Optically Pumped by a TEA CO_2 Laser", M.S. Thesis, University of Illinois, Urbana, IL (1977).

II. SUPERFLUORESCENT EMISSION BY TWO-PHOTON PUMPING $^{14}NH_3$ - William Lee

I. Introduction

Two-photon pumping and higher order processes have been shown[1] to be attractive in that there are more accessible levels, larger saturation intensity and more processes involved, than the single-photon pumping. Although two-photon pumping in $^{14}NH_3$ has been studied previously,[2,3] in this section, we report the first observation of superfluorescent emissions in $^{14}NH_3$ by such process.

A Pyrex capillary tube was used as a dielectric waveguide to confine the intense pumping radiation provided by the CO_2 TEA lasers. P(24) (10μm) and P(34)(9μm) lines of the CO_2 laser counter-propagating inside the capillary tube, generates the superfluorescent emission at 12.18 μm. Another superfluorescent emission at 35.13 μm was also generated by P(24) (10μm), where the two photons are of the same energy.

II. Experiments

Two synchronized single mode CO_2 TEA lasers, triggered by hydrogen-thyrotron to reduce jittering of the laser pulses, provide the pumping radiations P(34) (9μm) and P(24) (10μm) for the first scheme (Fig. 1) of the two-photon pumpings in $^{14}NH_3$. Linearly polarized perpendicular to each other, these two pumping radiations counter-propagate inside a 3 mm bore

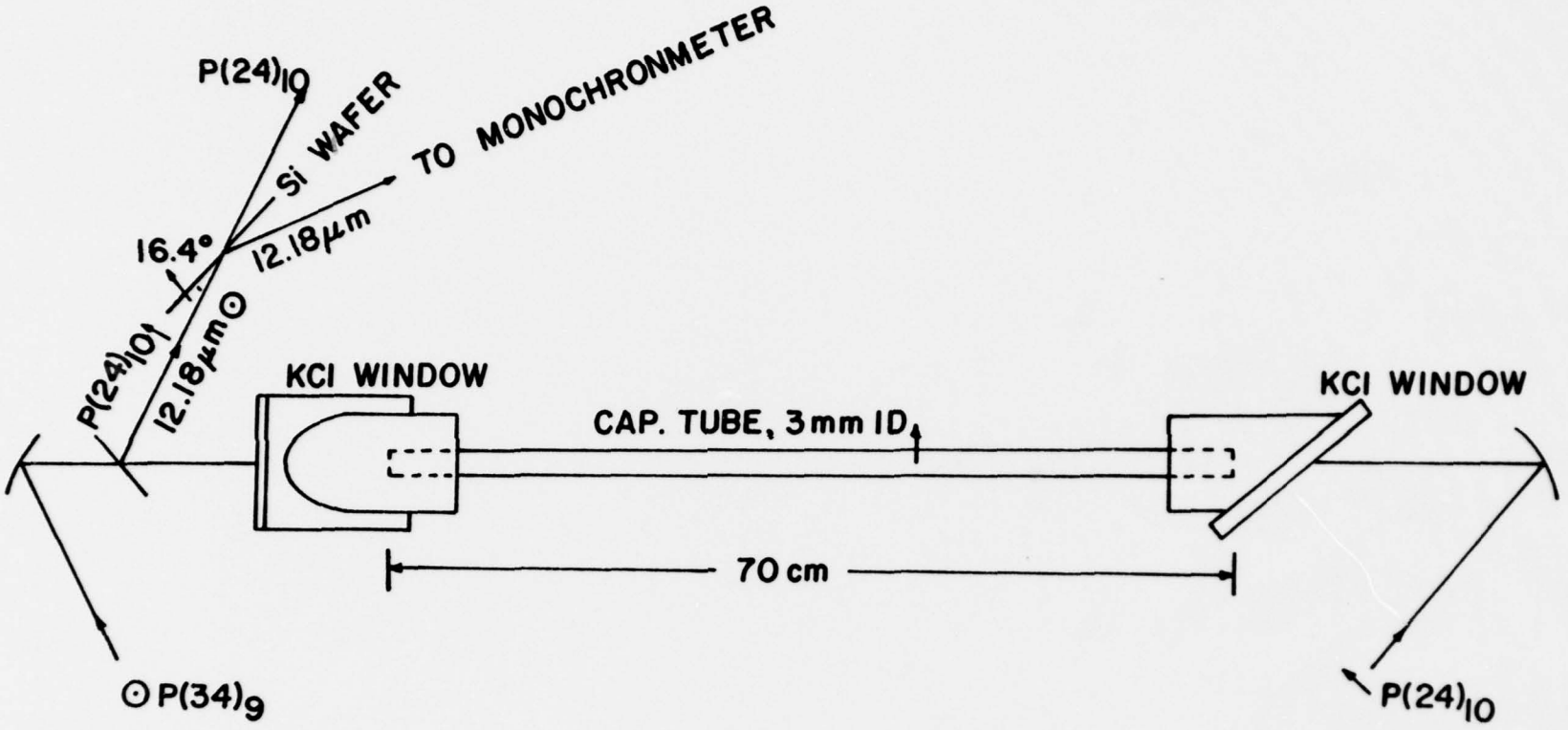

Figure 1. Superfluorescent emission 12.18 μm generated by two-photon pumping $^{14}NH_3$ inside capillary tube.

Pyrex capillary tube of length 70 cm. The capillary tube serves as a dielectric waveguide to preserve the intensities ($\sim$ 10 mW/cm^2) of the focused radiations. The superfluorescent emission at 12.18 μm generated by two-photon pumping, was separated from the pumping line p(24) (10μm) with a Si wafer placed at Brewster angle (16.4°) with respect to the pump polarization. The Si wafer reflected 90% of the signal which was sent through a monochronmeter for detection.

The same two-photon pumping also generates another emission at 26.71 μm from a two-holed cavity (Fig. 2-A). Polarized as the first experiment, those two pumping radiations were combined and then focused into the 1m long cavity. The cavity was made of a curved mirror, of 2m focus length and 2.0 mm center hole, and a flat mirror of 0.5 mm center hole. The signal and pumps from the cavity were filtered by a 12 μm filter (dielectric coated Ge) before detected via a monochronmeter.

The third experiment (Fig. 2-B) utilized the same capillary tube as in Fig. 1, but with a mode-locked CO_2 TEA laser to provide P(24) (10μm) for the two photons of the same energy. The superfluorescent emission at 35.13 μm was detected after being filtered through the high density polyethylene and the monochronmeter.

III. Results and Discussion

III-1 12.18 μm and 26.71 μm

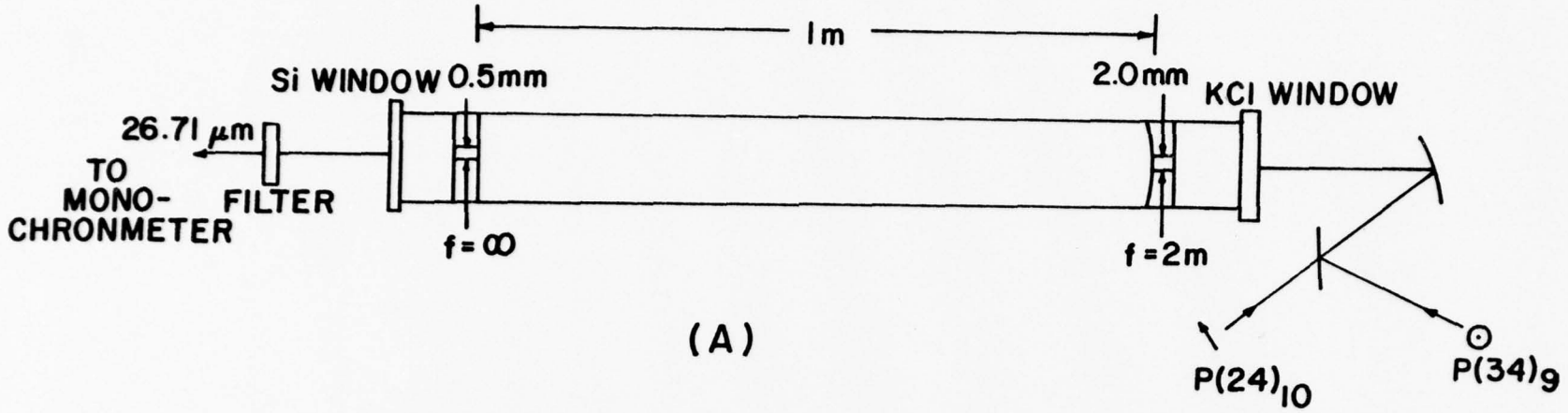

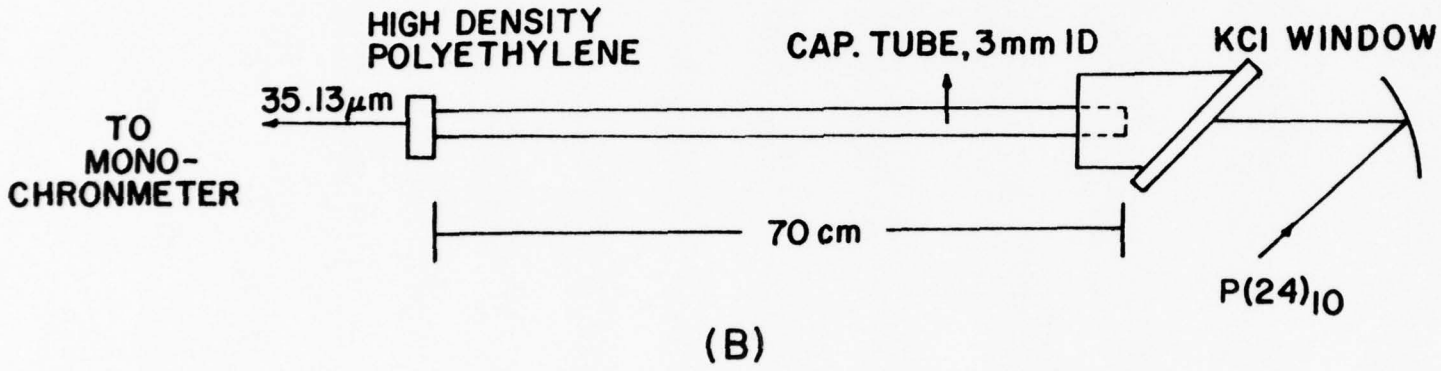

Figure 2. (A) 26.71 μm generation from two-photon pumping $^{14}NH_3$ in a cavity. (B) Superfluorescent emission 35.13 μm generated by two-photon pumping $^{14}NH_3$ inside capillary tube.

In the first two experiments, the two-photon pumpings were assigned as shown in Fig. 3. The two-photon transition from the ground vibrational state Ga(4,2) to the second vibrational state $2\nu_2$a(5,2) is matched by the two pumps P(34) (9μm) and P(24) (10μm) of CO_2 lasers. The total energy mismatch[4] is 0.0046 cm^{-1} while the intermedium mismatch is 0.1727 cm^{-1}. Both mismatches are of the same order as the two-photon pumping by Jacobs et al.[3] The changes of J values that $\Delta J = 1$ of Ga(4,2) → ν_2s(5,2) and $\Delta J = 0$ of ν_2s(5,2) → ν_2a(5,2) required the two pumps polarized perpendicular to each other.[5] Following the two-photon transition, the superfluorescent emission at 12.18 μm was assigned as $2\nu_2$a(5,2) → ν_2s(6,2) while the emission at 26.71 μm was assigned as $2\nu_2$a(5,2) → $2\nu_2$s(4,2). The pressure dependences of 12.18 μm were plotted in Fig. 5 and 26.71 μm in Fig. 6.

III-2. 35.13 μm

In the third experiment, the $^{14}NH_3$ pressure dependence of the superfluorescent emission is shown in Fig. 7. Peak signal appreared at 32 torr, indicative of a hot band, single photon absorption, rather than two-photon pumping. In the assignement (Fig. 4), the overall two-photon mismatch is 0.0195 cm^{-1}, but the intermediate mismatch is 8.9171 cm^{-1}, a rather larger value. However, the pump mode-locked intensities are quite large, so that a two-photon absorption is highly probable. The large intermediate mismatch will mean

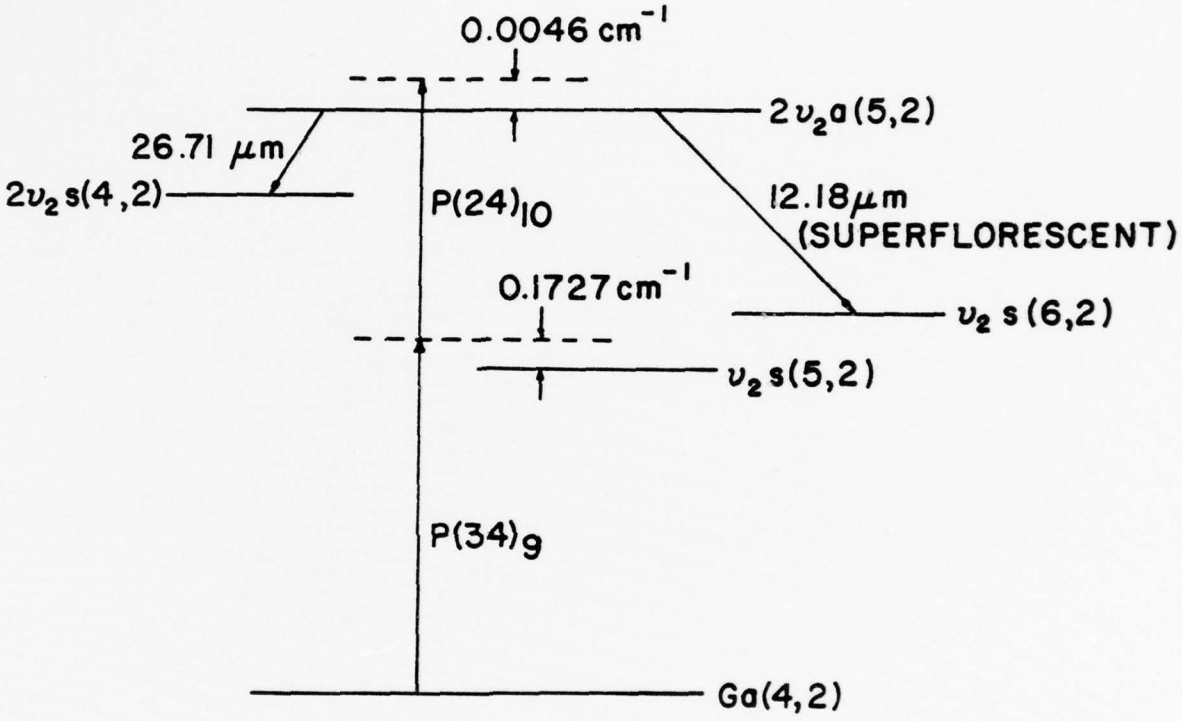

Figure 3. Two-photon pumping assignment for generations of 12.18 μm and 26.71 μm in $^{14}NH_3$.

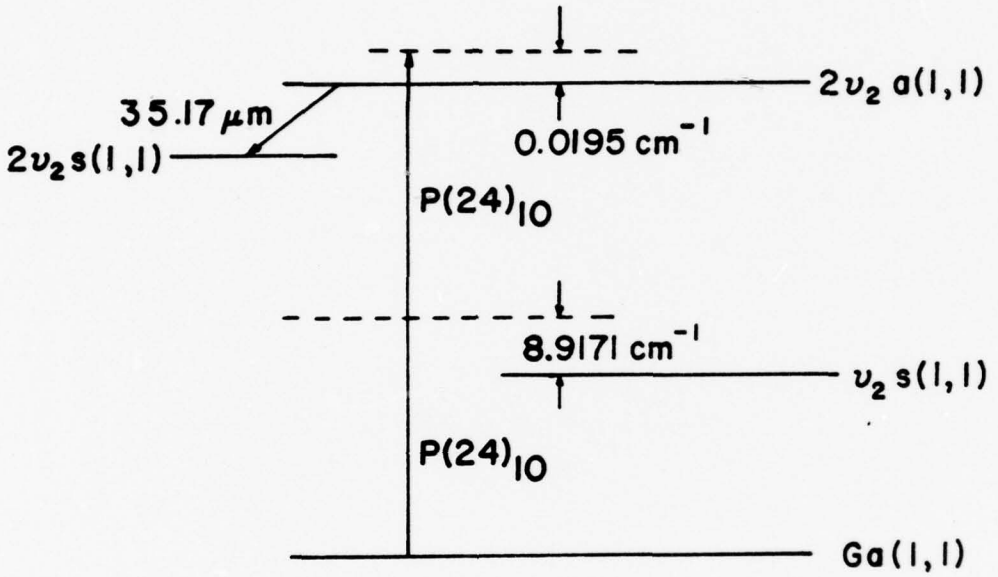

Figure 4. Two-photon pumping assignment for generation of 35.17 μm in $^{14}NH_3$.

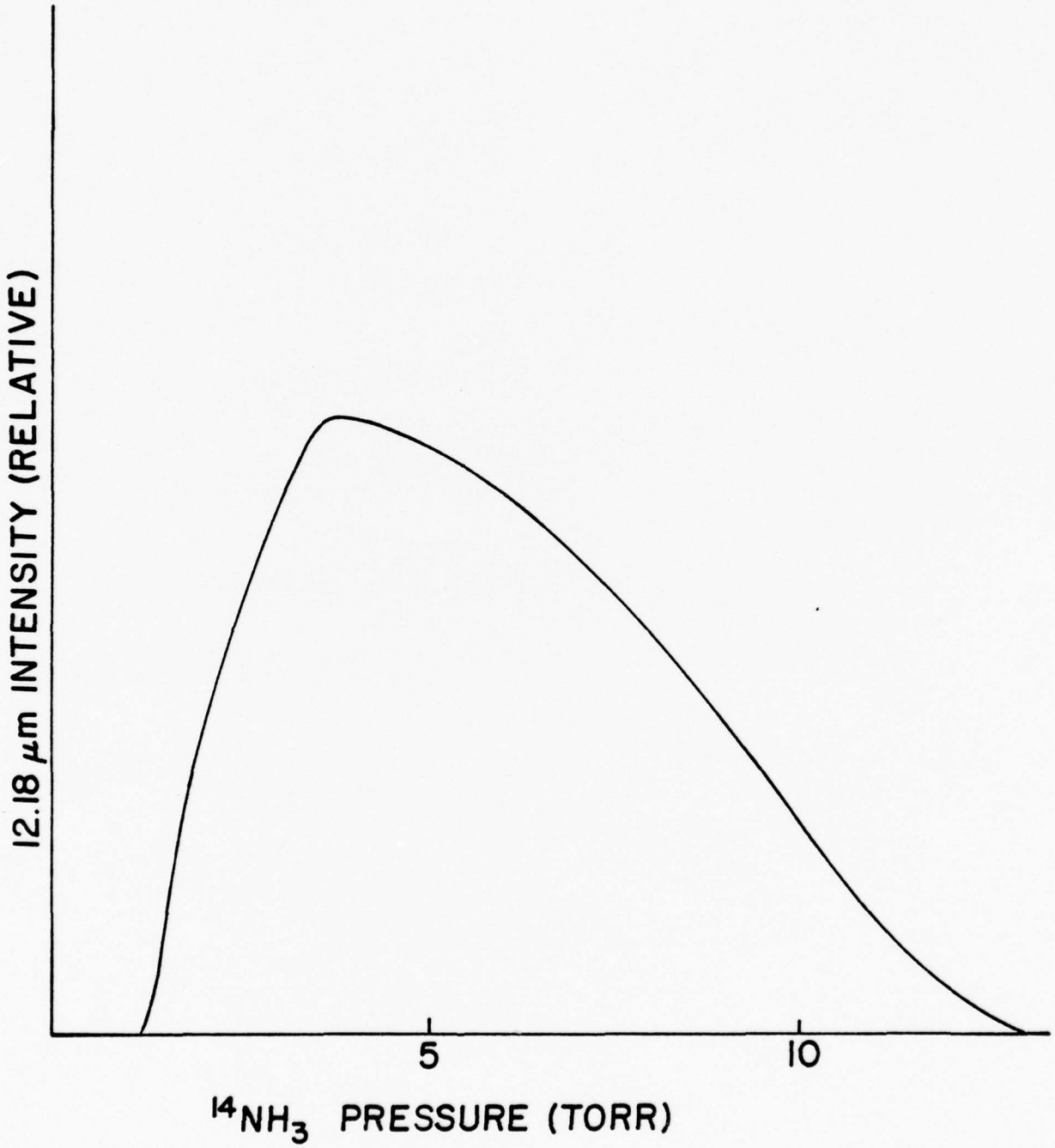

Figure 5. $^{14}NH_3$ pressure dependence of superfluorescent emission 12.18 μm.

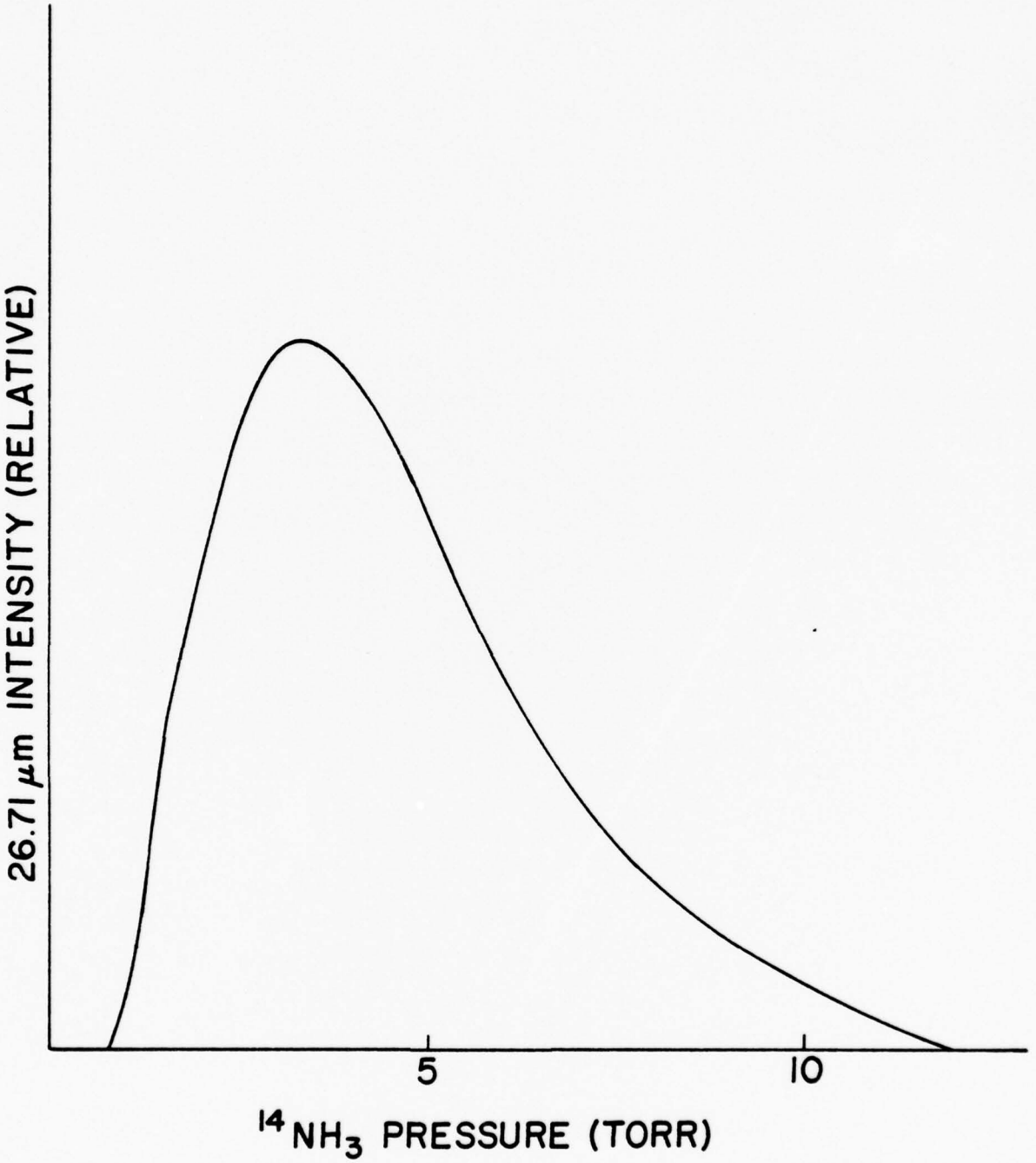

Figure 6. $^{14}NH_3$ pressure dependence of emission 26.71 μm.

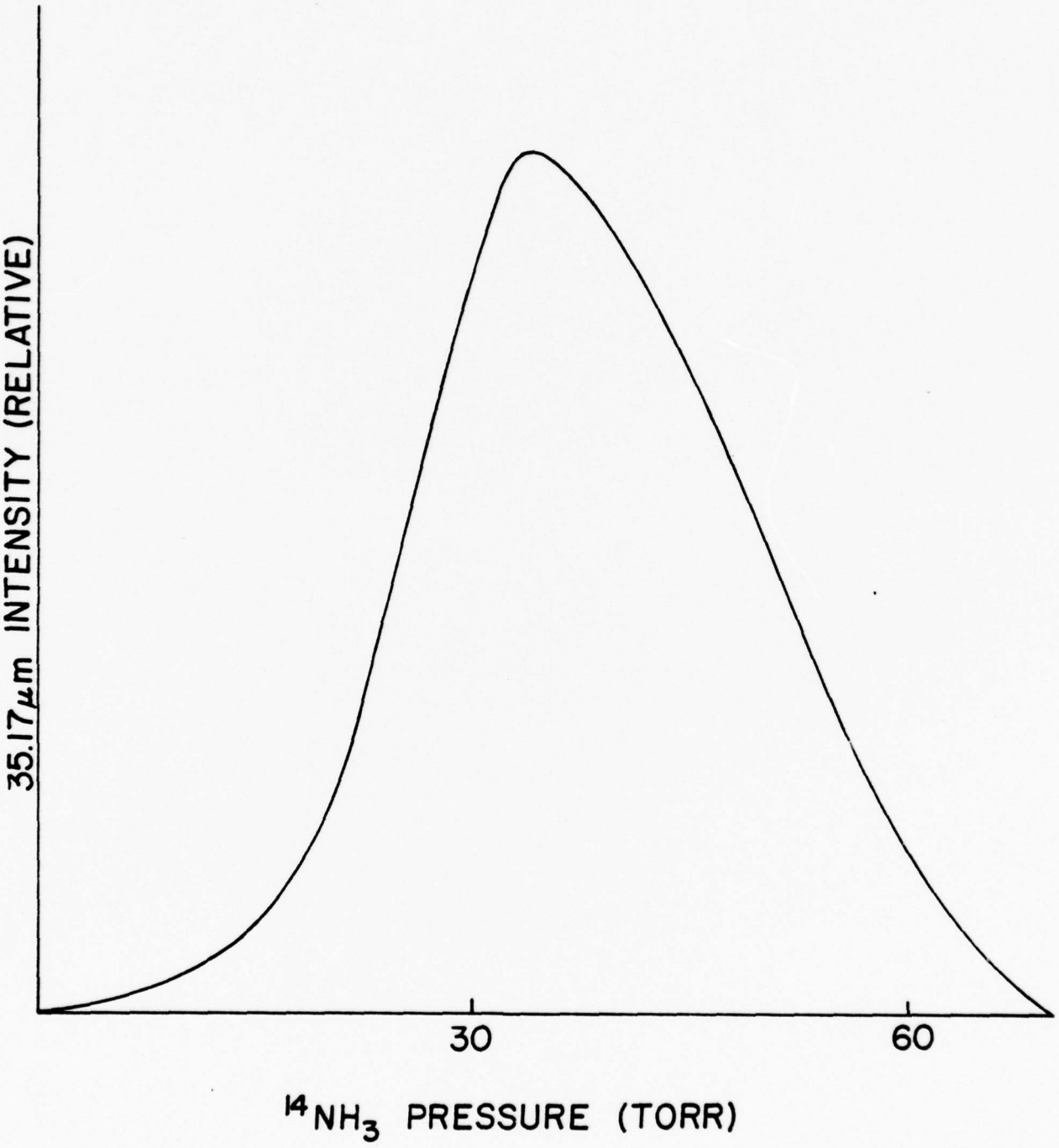

Figure 7. $^{14}NH_3$ pressure dependence of superfluorescent emission 35.17 μm.

that the intermediate level $\nu_2 s(1,1)$ is not appreciably populated. Many other assignments were considered, but the best fit was the $Ga(1,1) - \nu_2 s(1,1) - 2\nu_2(1,1)$ followed by the emission $2\nu_2 a(1,1) - 2\nu_2 s(1,1)$

IV. Conclusions

Two superfluorescent emission of 12.17 μm and 35.13 μm have been generated by two-photon pumping ν_2 band of $^{14}NH_3$ with CO_2 TEA lasers. Compared to the ground state single photon pumping, the less probable two-photon processes attributed to employment of the capillary tube as a dielectric waveguide. The accessibility of the second vibration rung of $^{14}NH_3$, demonstrated that new lasing frequencies could be generated with present "winner" molecules pumped by various combinations of CO_2 laser lines. Higher order effects could also be exploited, i.e., hyper-Raman lasers and parametric mixing.

References

1. P. D. Coleman, "Hyper-Raman Scattering", Paper D-1, LASERS '78 International Conference, Orlando, Florida, December 1978.

2. J. W. Leap, et al., "Two-photon Pumping of a Four-Level System", Paper C6.1, 1978 IEEE MTT-S International Microwave Symposium, Ottawa, Canada, June 1978.

3. R.R. Jacobs, et al., "Laser Generation from 6-35 μm Following Two Photon Excitation of Ammonia", Appl. Phys. Lett., vol. 29, pp. 710-712, December 1976.

4. J. Curtis, "Vibrational-Rotational Bands of NH_3 in the 67° to 1860 cm^{-1} Region", Ph.D. Dissertation, The Ohio State University, 1974.

5. T. Y. Chang, IEEE Trans. Microwave Theory Tech. MTT-22, p. 983, 1974.

III. HYPER-RAMAN SCATTERING STUDIES IN $^{14}NH_3$ - David Kim

I. Introduction

The research on the optical pumping of IR molecular lasers has been mostly single pump, two-photon processes which yield either a laser or a Raman signal.

Multiple photon pumping of molecules would show many interesting non-linear phenomena as well as generating many new lines. Our density matrix analysis for the two-photon pumping shows laser, Raman and hyper-Raman gain simultaneously. The first stimulated hyper-Raman scattering in the visible was observed by S. Yatsiv et al. in K-vapor.[1] Efficient tunability was demonstrated by D. Cotter et al. in Na-vapor.[2] Yu. A. Il'inskii, et al. estimated hyper-Raman gain coefficient using density matrix theory. Their result predicts hyper-Raman gain can be increased considerably by pumping with infrared frequency laser (e.g., CO_2 laser).[3] Our analysis of two-photon pumping using density matrix theory, shows that the hyper-Raman process has a larger saturation, yields more output power and has less a.c. Stark shift than the laser and Raman processes. Our objective is identifying the hyper-Raman gain peak by probing the gain peaks. The following three different cases are the candidates (Fig. 1).

II. Theory and Calculation

Various combinations of three-photon, three-or four-level

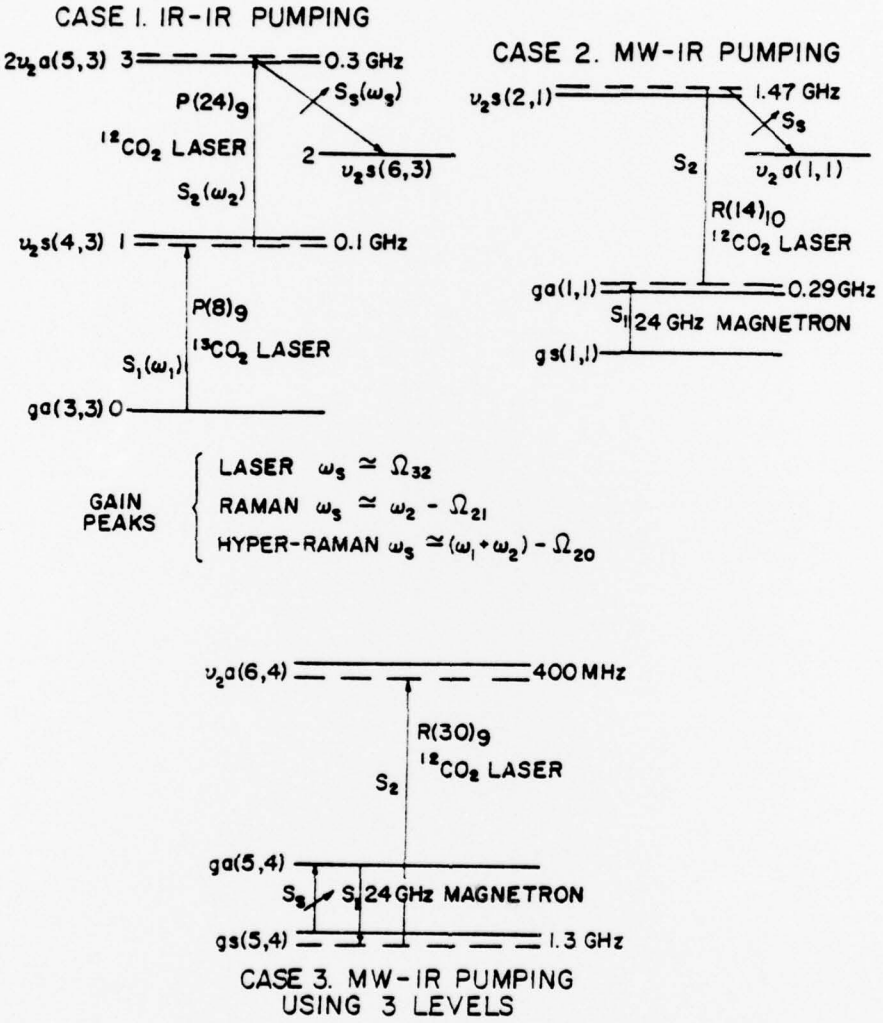

Figure 1. Examples of three-photon systems in $^{14}NH_3$.

systems were studied by using a density matrix analysis.

The density matrix equations,

$$\frac{\partial \rho_{nn}}{\partial t} + \frac{\rho_{nn} - \rho^{e}_{nn}}{(T_1)_m} = \frac{1}{ih} \sum_k \left(H'_{ne}\rho_{kn} - \rho_{nk}H'_{nk} \right) \qquad (1)$$

$$\frac{\partial \rho_{mn}}{\partial t} + \left(\frac{1}{(T_2)_{mn}} - i\Omega_{nm} \right) \rho_{mn} = \frac{1}{ih} \sum_{m,k} \left(H'_{mk}\rho_{kn} - \rho_{mk}H'_{kn} \right) \qquad (2)$$

are used with the following assumptions,

1. steady state
2. homogeneous line widths
3. rotating wave approximations
4. one simple relaxation times T_1 and T_2 for each vibrational state
5. sharp pump frequency.

One cannot use an iterative approach, because the coupling terms can be big when the signals start to saturate. The whole 16 linear complex equations must be solved simulataneously for each M-level and averaged over the initial state. The density matrix element $\rho_{23} = \lambda_3 e^{i\omega_s t}$ is the element of interest from which the electrical susceptibility χ_e can be calculated, i.e.,

$$\varepsilon_o \chi_e = \varepsilon_o (\chi'_e - i\chi''_e) = \frac{2N\mu_{23}\lambda_3}{E_s}$$

where ε_o is the free space permitivity, N is the molecular density, μ_{23} the dipole matrix element associated with levels 2

and 3, and E_s is the signal field. A partial analytical solution of the Equations (2) can be found in terms of the steady state (ρ°_{nn}) values of the diagonal elements in the form

$$\frac{\hbar R_3}{iN|\mu_{23}|^2 T_2}\,\varepsilon_o \chi_e = \left(1 - \frac{b^2}{\delta_1}\left(\frac{1}{R_1^*} + \frac{1}{R_3}\right) + \frac{a^2 b^2}{\delta_2 R_2^*}\right)(\rho^{\circ}_{33} - \rho^{\circ}_{22})$$

$$+ \left(\frac{b^2}{\delta_1 R_2^*} - \frac{a^2 b^2}{\delta_2}\left(\frac{1}{R_1^*} + \frac{1}{R_2^*}\right)\right)(\rho^{\circ}_{11} - \rho^{\circ}_{22}) \qquad (3)$$

$$+ \left(\frac{a^2 b^2}{\delta_2 R_1^*}\right)(\rho^{\circ}_{00} - \rho^{\circ}_{22})$$

where the normalized fields are,

$$a = \frac{\mu_{01} E_1 T_e}{2h}\,, \qquad b = \frac{\mu_{13} E_2 T_2}{2h}\,, \qquad c = \frac{\mu_{23} E_s T_2}{2h}$$

and the resonant demoninators are

$$R_1 = 1 + iT_2(\omega_1 - \Omega_{10}) \quad \text{and} \quad R_2 = 1 + iT_2(\omega_2 - \Omega_{31})$$

with δ_1 and δ_2 complicated resonance terms containing the a^2, b^2 and c^2, plus the variable frequency term $R_3 = 1 + iT_2(\omega_s - \Omega_{32})$. It is seen from Equation (3) that the gain $g_s = -\omega_s \chi_e''/v_g$, where v_g is the group velocity, has three contributing terms: one proportional to $(\rho^{\circ}_{33} - \rho^{\circ}_{22})$ the laser term, one proportional to $(\rho^{\circ}_{11} - \rho^{\circ}_{22})$ the Raman term, and one proportional to $(\rho^{\circ}_{00} - \rho^{\circ}_{22})$ the hyper-Raman term.

To display the saturation behavior, the peaks in the laser, Raman and hyper-Raman gains versus signal intensity S_s, have been plotted in Fig. 2. For a threshold gain of the order of 0.004, it is seen that hyper-Raman process contributes almost two orders of magnitude in signal power density. The experiment for the case I provides the opportunity to test the theory. A 0.5 millijoule, 0.5 μsec signal was generated by two-photon pumping in NH_3 at 12.159 μm. A 70 cm long, hole coupled (area = $10^{-2}cm^2$) resonator was used.

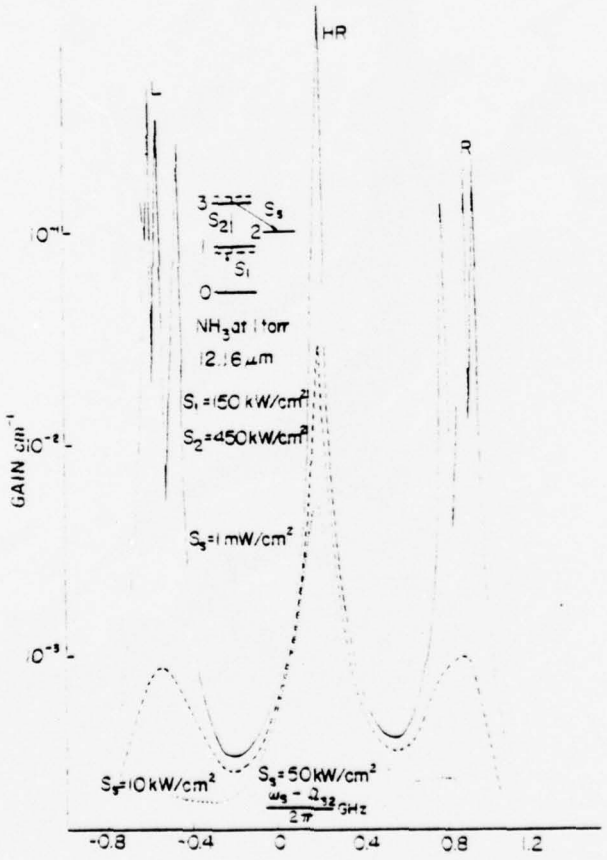

Figure 2. Gain spectrum curves displaying M-level splitting and gain saturation with signal intensity for Case 1.

Assuming the field intensity in the hole aperture was the same as in the laser cavity, one could estimate the signal intensity as

$$S_s \cong \xi_s/(\text{area}\cdot\Delta\tau) = 5\times10^4/(10^{-2})(5\times10^{-7}) \cong 100 \text{ kW/cm}^2$$

From our computer calculation, this signal intensity yields a gain of g_s of 0.0032 cm^{-1}. A signal gain of this value would in turn yield a loss per pass $\alpha_T = bg_s = 70(0.0032) = 0.21$ and a resonator $Q = \frac{2h}{g_s\lambda_s} = 2\pi/)0.0032)(12.159\ 10^{-4}) \cong 1.6\times10^6$. Thus the calculations are self-consistent and yield appropriate values for expected experimental quantities.

In Fig. 3, a typical gain curve is plotted versus the signal frequency offset for the IR-IR pumping case. A two-photon energy match is assumed with a variable intermediate match to level 1. The curve for $\delta = 0$ (intermediate mismatch) shows the laser-Raman splitting of the gain, equally spaced on either side of the system resonant, while the hyper-Raman gain peaks at line center. As the intermediate match is varied, from $\delta = 1$ to $\delta = 10$ GHz, the peak in the laser gain contribution moves towards line center, the Raman gain contribution moves further away from the line center, while the hyper-Raman remains on the line center.

In Fig. 4 the gain curve for the case 2 is shown.

III. Experimental Progress

Three different types of transition combinations can be

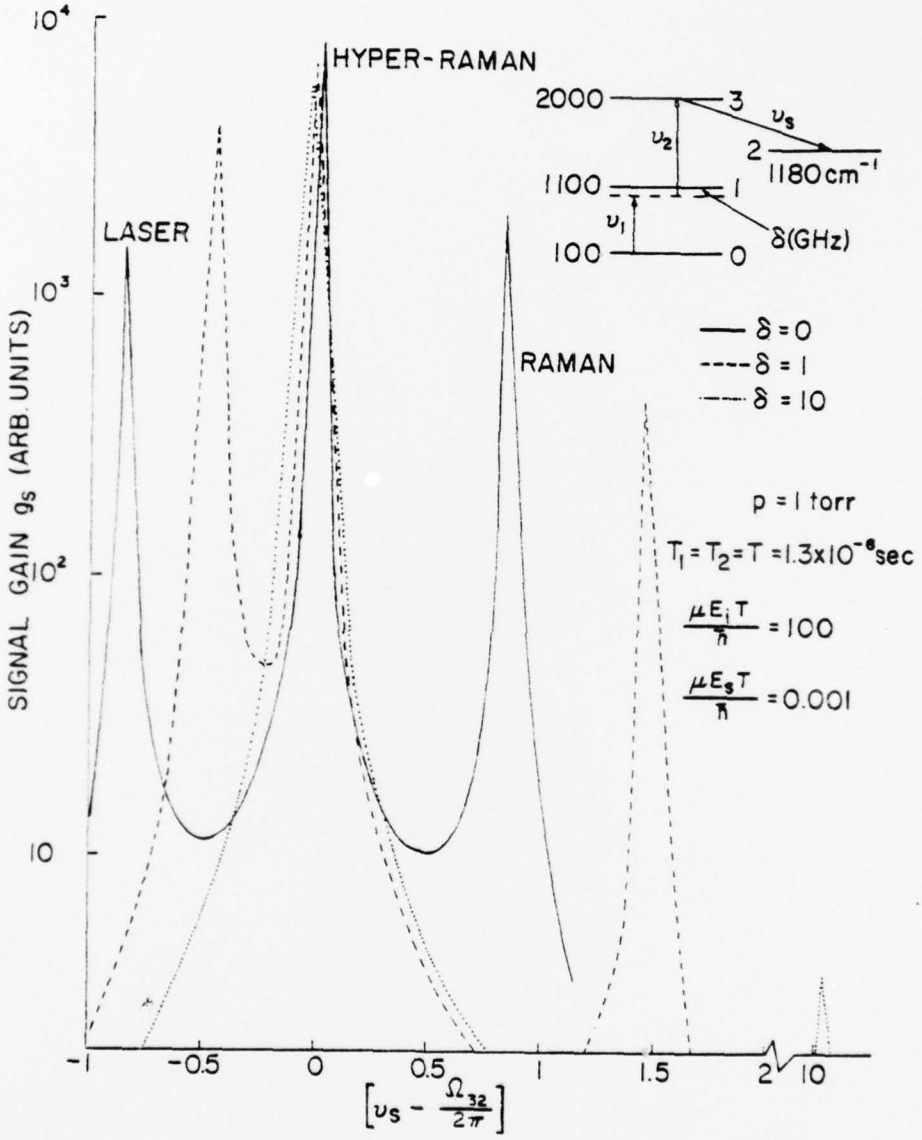

Figure 3. Gain curves displaying the effect of intermediate level mismatch.

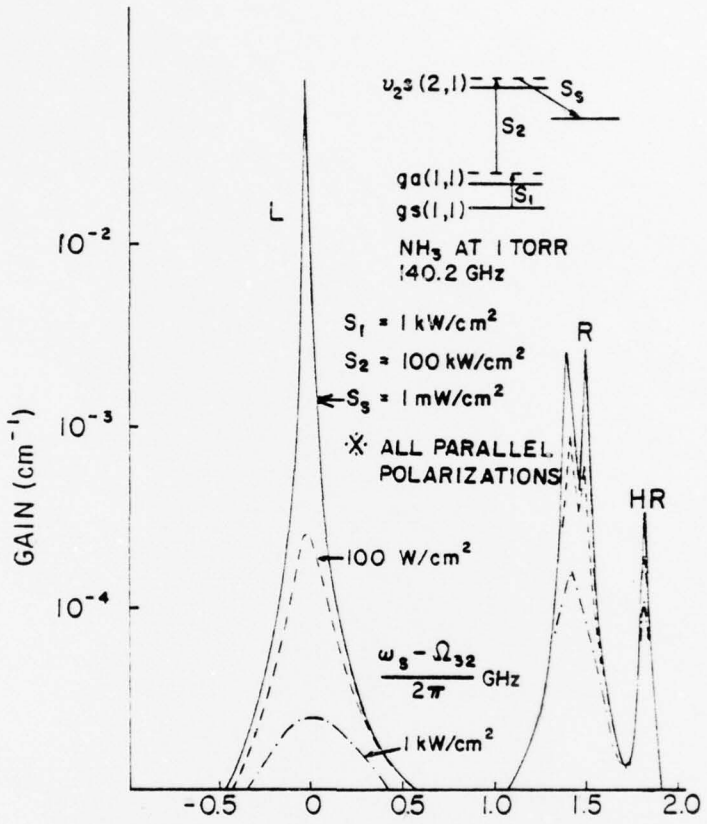

Figure 4. Microwave and CO_2 laser pump gain.

used to find laser, Raman and hyper-Raman gains. These schemes are shown in Fig. 5. Many similar transitions are found for each case.

Case 1

TRANSITIONS	PUMP LASER	OVERALL OFFSET	INTERMEDIATE OFFSET
gaQ(5,4)	$P(18)_{10\mu}$ CO_2	0.294GHz	5.25GHz[5]
ν_2sQ(5,4)	$P(34)_{10\mu}$ CO_2		
gaR(1,1)	$R(14)_{10}$ CO_2	1.2 GHz	1.5 GHz
ν_2sR(2,1)	$P(14)_9$ $^{13}CO_2$		
gaQ(5,3)	P(7) N_2O	4 MHz	3.3 GHz
ν_2sQ(5,3)	R(4) N_2O		
gaQ(5,3)	$P(32)_{10}$ CO_2	1.63 GHz	0.93GHz
ν_2sR(5,3)	$P(16)_9$ CO_2		

Case 3[6]

TRANSITIONS	PUMP LASER	LASER OFFSET	INVERSION SPLITTING
gaQ(8,6)	$P(34)_{10}$ CO_2	3.6 GHz	20.73GHz
gaQ(8,7)	P(13) N_2O	2 MHz	23.23GHz
gsQ(5,4)	$R(6)_{10}$ CO_2	0.544GHz	22.65GHz
gsQ(2,2)	$R(8)_{10}$ CO_2	9.926GHz	23.72GHz

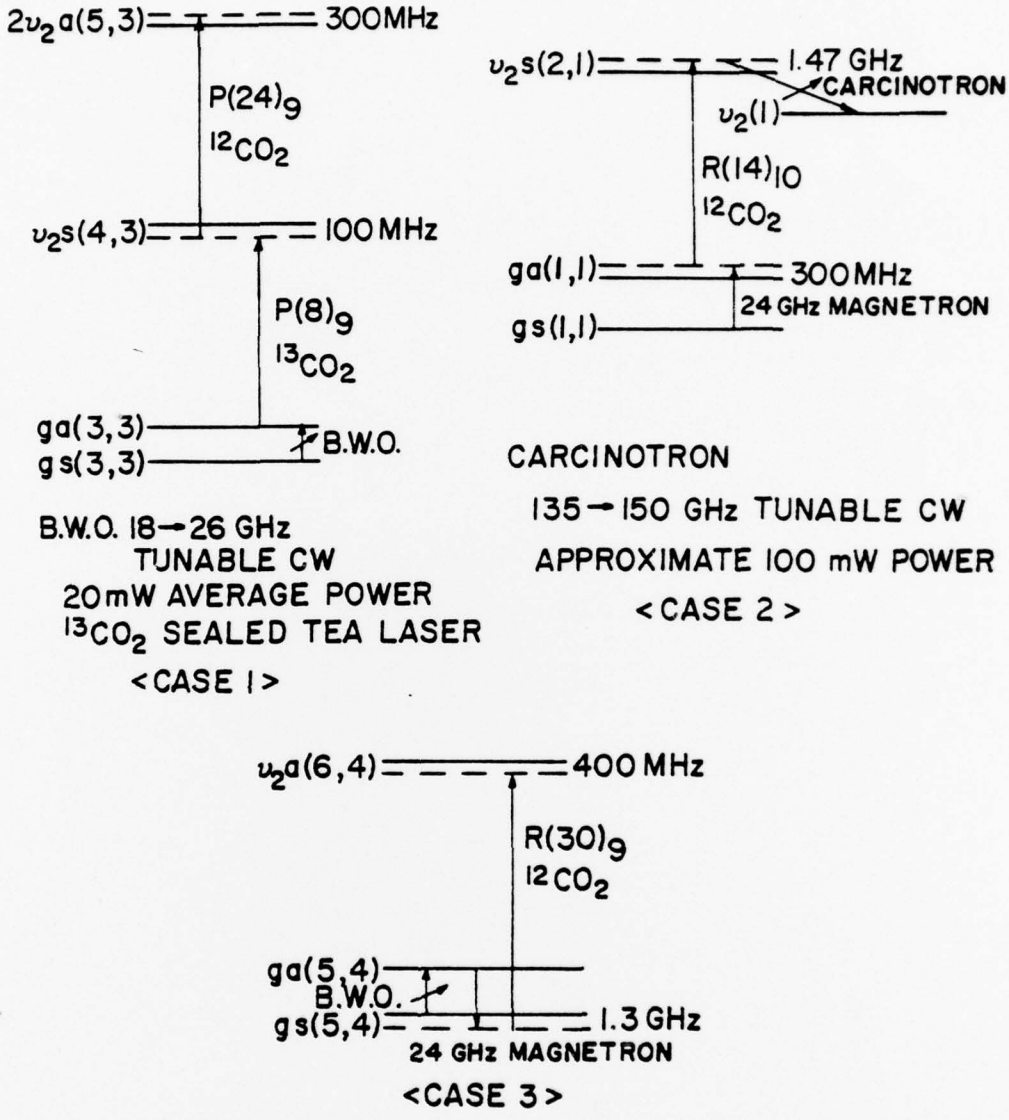

Figure 5. Raman or hyper-Raman gain probe schemes.

The experimental scheme for the Case 1 which measures three-photon absorption is equivalent to the hyper-Raman process in Fig. 1. The waveguide cell will be essentially the same as that of H. Jones[8]. In Case 2, mixing 140 GHz with 24 GHz is done by Teflon prism.[7] It reflects over 80% of the short wavelength signal to the 90° direction while transmitting most of the long wavelength signal through. The oversized waveguide for 140 GHz signal could be too lossy to detect the gain of the probling signal. In case 3, separating the probing signal from the magnetron signal must be done by an appropriate filter.

References

1. S. Yatsiv, et al., IEEE JQE, p. 900 (1968).
2. D. Cotter, et al., Opt. Comm. 22, p. 190 (1977).
3. Yu. A. Ilinskii, et al., Sov. JQE, 4, p. 997 (1975).
4. P.D. Coleman, Laser Conference 1978, Orlando, Fla. Paper D-1, December (1978).
5. R. Jacobs, et al., Appl. Phys. Lett. 29, p. 710 (1976).
6. S. M. Freund and T. Oka, PRA, 13, #6, p. 2178 (1976).
7. R. G. Fellers, et al., IEEE TMTT, p. 587 (1964).
8. H. Jones, Appl. Phys. 14, p. 169 (1977).

IV. PERSONNEL ASSOCIATED WITH GRANT AFOSR 76-2988

	Percent of Time	Period
P.D. Coleman, Professor Principle Investigator	10%	August 21, 1978 - January 5, 1979
	70%	May 21, 1978 - July 20, 1978
Edward G. Malk Research Assistant	50%	February 1, 1978 - January 31, 1979
William Lee Research Assistant	50%	February 1, 1978 - January 31, 1979
David Kim Research Assistant	50%	April 21, 1978 - January 31, 1979
John Leap Research Assistant	50%	February 1, 1978 - April 20, 1978
Robert Miller Research Assistant	25%	January 6, 1979 - January 31, 1979
Joseph Niesen Research Assistant	17%	February 1, 1978 - May 20, 1978
Donald S. Fulton Electronics Technician	25%	February 1, 1978 - January 31, 1979
Jimmie Smith Secretary	20%	February 1, 1978 - January 31, 1979

V. TECHNICAL ACTIVITIES - Principle Investigator

1. Presented invited paper, "Hyper-Raman Scattering", Lasers'78 Conference, Orlando, Florida, December, 1978.

2. Attended and presented paper, "Laser Emission in the 83-223 μm Region from PH_3 with Laser Line Assignments", 3rd International Submillimeter Wave Conference, Guildford, England, March 1978.

3. Presented paper, "Two-photon Pumping of a Four-Level System in Ammonia to Obtain 12.16 μm Radiation for Isotope Separation", 1978 IEEE MTT International Microwave Symposium, Ottawa, Canada, June 1978.

4. Treasurer, Device Research Conference, 1967-present.

5. Member URSI Commission I.

6. Review papers for Applied Phys. Lett., IEEE-MTT, Journal of Quant. Electron., Journal of Appl. Phys.

7. Review proposals for National Science Foundation and Army Research Office.

8. Visited Minneapolis, MN, Honeywell, July 1978.

9. Visited Rockwell International and gave seminar, "Laser Emission in the 83-223 μm Region from PH_3 with Laser Line Assignments" at the University of Southern California, February 1978.

10. Attended CLEOS Conference, San Diego, CA, February 1978.

11. Associated Editor - Journal of Quantum Electronics.

12. Presented paper, Annual Review of Electronics, University of Illinois, "Hyper-Raman Scattering", October 1978.

13. Member Joint Physical Society, IEEE Journal of Quantum Electronics.

VI. MANUSCRIPTS SUBMITTED TO JOURNALS

1. "Laser Emission in the 83-223 μm Region from PH_3 with Laser Line Assignments", with E. Malk, J. Niesen, and D. Parsons, IEEE J. Quant. Electron., QE-14, 544, July 1978.

2. "Hyper-Raman Scattering and Related Phenomena", Lasers '78 Conference, SPIE, January 1979.

3. "Hot Band Lasing in NH_3" with W. Lee, D. Kim, E. Malk, and J. Leap, submitted to the Journal of Quantum Electronics.

VII. THESES

1. "A Phosphine Far Infrared Laser Optically Pumped by a Transverse Excitation Atmospheric Pressure Carbon Dioxide Laser', Joseph W. Niesen, M.S. Thesis, University of Illinois, 1978.